AEM Accepted Manuscript Posted Online 13 July 2018
Appl. Environ. Microbiol. doi:10.1128/AEM.00950-18










# Quorum sensing in *Pseudomonas savastanoi* pv. *savastanoi* and *Erwinia toletana*: role in virulence and interspecies interactions in the olive knot

Eloy Caballo-Ponce[1]*, Xianfa Meng[2]*[¶], Gordana Uzelac[2], Nigel Halliday[3], Miguel Cámara[3], Danilo Licastro[4], Daniel Passos da Silva[2‡], Cayo Ramos[1+], and Vittorio Venturi[2+]

Instituto de Hortofruticultura Subtropical y Mediterránea La Mayora, Universidad de Málaga-Consejo Superior de Investigaciones Científicas, Málaga, Spain[1]

International Centre for Genetic Engineering and Biotechnology, Trieste, Italy[2]

School of Life Sciences, Centre for Biomolecular Sciences, University of Nottingham, Nottingham, United Kingdom[3]

CBM S.c.r.l., Area Science Park-Basovizza, Trieste, Italy[4]

* equal contribution

+ co-corresponding - Vittorio Venturi, email: venturi@icgeb.org; Cayo Ramos, email: crr@uma.es

¶ current address: Integrative Microbiology Research Centre, South China Agricultural University, Guangzhou 510642, China

‡ current address: Department of Microbiology, University of Washington, Seattle, WA.

**ABSTRACT:** The olive-knot disease (*Olea europea* L.) is caused by the bacterium *Pseudomonas savastanoi* pv. *savastanoi* (PSV). PSV in the olive-knot undergoes interspecies interactions with the harmless endophyte *Erwina toletana* (ET); PSV and ET co-localize and form a stable community resulting in a more aggressive disease. PSV and ET produce the same type of the *N*-acylhomoserine lactone (AHL) quorum sensing (QS) signal and they share AHLs in planta. In this work we have further studied the AHL QS systems of PSV and ET in order to determine possible molecular mechanism(s) involved in this bacterial inter-species interaction/cooperation. The AHL QS regulons of PSV and ET were determined allowing the identification of several QS-regulated genes. Surprisingly, the PSV QS regulon consisted of only a few loci whereas in ET many putative metabolic genes were regulated by QS among which several involved in carbohydrate metabolism. One of these loci was the aldolase-encoding gene *garL*, which resulted to be essential for both co-localization of PSV and ET cells inside olive knots as well as knot development. This study further highlighted that pathogens can cooperate with commensal members of the plant microbiome.

**SIGNIFICANCE OF THIS STUDY:** This is a report on studies of the quorum sensing (QS) systems of olive knot pathogen *Pseudomonas savastanoi* pv. *savastanoi* and olive-knot cooperator *Erwinia toletana*. These two bacterial species form a stable community in the olive knot, share QS signals and cooperate resulting in a more aggressive disease. In this work we further studied the QS systems by determining their regulons as well studying QS-regulated genes which might play a role in this cooperation. This represents a unique in vivo interspecies bacterial virulence model and highlights the importance of bacterial interspecies interaction in disease.

## INTRODUCTION

The recent dramatic increase of microbiome studies has further evidenced what microbiologists have postulated for many years, that most commonly, microorganisms in nature live as members of complex multispecies communities (1, 2). This has demonstrated that many different microbes live in close proximity to each other; however, aspects of microbe-microbe interactions have thus far been significantly understudied. In addition, multispecies microbial communities existing in association with plants could be influenced by the plant and/or could have consequences on plant health; again very few studies have investigated this likely scenario.

Many bacterial species have been studied for their intraspecies signaling system which is known as quorum sensing (QS) (3). QS involves the production and detection of signal molecules which results in the regulation of gene expression in response to bacterial cell number/density (4). Gram-negative bacteria most commonly use *N*-acylhomoserine lactones (AHLs) as QS signals and in proteobacterial phytopathogens it is involved in the regulation of expression of virulence associated factors in the plant (5-9). An archetypical AHL QS system consists of a LuxI-family AHL synthase and a LuxR-family transcription factor which affects target gene expression upon interaction with the cognate AHL at quorum concentrations (10). AHLs vary in their structure having different acyl chain lengths (from 4 to 20 carbons) and display differences in their oxidation state at position C3. AHL signals can also be involved in interspecies signaling in a community since they are freely diffusible and can thus be detected by different bacterial neighbors. In bacterial pathogenesis, especially in human hosts, it is now becoming recognized that many pathogens interact with other microorganisms which may influence the disease process (11-13).

Plant microbial diseases are however still very much considered as being caused by single pure pathogens; nevertheless evidence is also beginning to grow that there can be synergisms between different microorganisms. Recently, a clear example of such synergism has been reported in the olive-knot disease of olive trees (*Olea europea* L.) caused by the bacterium *Pseudomonas savastanoi* pv. *savastanoi* (PSV) (14, 15). PSV possesses a typical LuxI/R AHL QS system and it is involved in virulence since mutants in this system result in significantly smaller knots (15). The bacterial load of the knots (also called tumors) is 50% composed of PSV but also contain a significant proportion of an apparently harmless commensal multispecies bacterial community (16) and some members have been shown to cooperate with PSV resulting in an increase of disease severity (15). More precisely, an *Erwinia toletana* (ET) strain (harmless to the olive plant) isolated from the olive knot increased disease severity (larger olive-knot) when co-inoculated with PSV. In addition, it was demonstrated that ET, *Pantoea agglomerans* and PSV form stable multispecies communities and that they share and communicate via AHLs. Interestingly, ET and PSV synthesize structurally identical AHLs and co-inoculation experiments have evidenced that *E. toletana* can rescue AHL negative mutants of PSV and restore virulence (15). Microscopy studies have also revealed that ET and PSV co-localize in the olive-knot further indicating that the two species are sharing the same niche both benefiting from this stable interaction. In addition, *in silico* recreation of the biochemical metabolic pathways encoded by PSV and ET genomes suggested that metabolic complementarity and/or sharing of metabolites could be involved in the beneficial interaction established between these two bacterial species (16). In this work we have further studied the AHL QS systems of PSV and ET, both *in vitro* and *in planta*, in order to identify specific molecular determinants involved in this interspecies bacterial interaction. Determination of the PSV and ET QS regulon allowed the identification of several QS-regulated genes putatively involved in numerous metabolic pathways, including the ET aldolase-encoding gene *garL*, which resulted to be essential for both co-localization of PSV and ET cells inside olive knots and full knot development.

## RESULTS

### The *luxI/R* quorum sensing genes in *Pseudomonas savastanoi* pv. *savastanoi* NCPPB 3335 and *Erwinia toletana* DAPP-PG 735

The olive knot pathogen *Pseudomonas savastanoi* pv. *savastanoi* (PSV) NCPPB 3335 (17, 18) was the first PSV genome sequenced and has been used in several studies of virulence mechanisms (19). This genome harbors a canonical *luxI*/*luxR* pair identical to the previously reported *pssI/R* QS system of PSV DAPP-PG 722 [hereafter named *pssI*/*pssR;* (15)] and two *luxR* solos which do not have a cognate *luxI* partner (Figure 1A). From the primary structure of the two LuxR solos, one likely responds to plant signals (designated as LuxR2) and the other most likely to AHLs (designated as LuxR3) (20, 21). Interestingly, this content of LuxI/R QS elements is conserved in all *P. savastanoi* strains infecting woody plants whose genomes have been sequenced (22-25).

With respect to the olive knot resident and PSV cooperator *E. toletana* (ET), we previously reported that ET DAPP-PG 735 was able to synthesize AHLs via the EtoI/R QS system. The *etoI* mutant, hereafter ETETOI, resulted in no AHL production hence it was concluded that ET possessed one AHL QS system (15). Sequencing of the ET genome (26) and its analysis performed here, surprisingly revealed that ET possessed a second complete canonical AHL QS system. The AHL-responsive transcriptional regulator gene was designated as *tolR* and the autoinducer synthase as *tolI* (Figure 1B).

### AHL production by *Pseudomonas savastanoi* pv. *savastanoi* NCPPB 3335 and *Erwinia toletana* DAPP-PG 735

QS and AHL production by PSV NCPPB 3335 has not been addressed so far, thus a *pssI* mutant and its complemented strain, expressing the *pssI* gene from a plasmid, were constructed. PSV NCPPB 3335, the *pssI* mutant and its complemented strain were grown overnight in LB broth and AHLs were extracted from spent supernatants as described in the materials and methods section. C6-AHL production was observed and determined for PSV NCPPB 3335, whereas no AHL production was detected for the Δ*pssI* mutant strain (Table 4 and S1). Interestingly, four types of AHLs (C6-, C8-, 3-oxo-C6- and 3-oxo-C8-AHLs) were identified in the supernatant of the Δ*pssI* complemented strain, indicating that overexpression of *pssI* leads to the production of some types of AHLs not detected in the wild type.

We also analyzed AHL production by the EtoI/EtoR and TolI/TolR ET DAPP-PG 735 QS systems. Production of six types of AHL was detected for the wild type ET DAPPG-PG 735: 3-oxo-C6-, 3-oxo-C8-, 3-oxo-C10-, C6-, C8- and 3-OH-C6-AHLs (Table 4 and S1). We previously reported that this ET strain produced 3-oxo-C6- and 3-oxo-C8-AHLs [15], thus this analytical chemical analysis revealed a wider spectrum of AHL production. As expected, the ETETOI mutant was unable to produce any type of AHL, while the ETETOI complemented strain restored the biosynthesis of all types of AHLs (Table 4 and S1). The ETTOLI showed a defect in the biosynthesis of 3-oxo-C10-AHL and unexpectedly it was not restored via the expression of *tolI* in trans. The summary of the complete AHL analysis in relation to the peak areas of the detected chromatographic peaks are provided in Table S1 and Figure S3.

**Transcriptional analysis of quorum sensing genes in PSV NCPPB 3335 and ET DAPP-PG 735**

We previously observed that a *pssR* mutant of PSV DAPP-PG 722 produced an amount of AHLs similar to the wild type strain, suggesting that the positive feedback loop typical of AHL QS systems does not occur in PSV. To address this possibility in PSV NCPPB 3335, the *pssI* promoter region was cloned in a promoter probe vector (pMP220) upstream a promoterless *lacZ* gene and β-galactosidase activity was measured in PSV NCPPB 3335 and its derivative *pssI* and *pssR* mutants during their growth. As shown in Figure 2A, the activity of *pssI* promoter was significantly increased in the stationary phase (10 hours incubation) compared to the exponential phase (4 hours incubation) in all three PSV genetic backgrounds. Moreover, no differences in β-galactosidase activity was observed among the three strains in neither log phase nor stationary phase, thus confirming that the typical AHL QS positive feedback loop does not occur in PSV NCPPB 3335.

It was also of interest to study the expression of the ET QS systems; gene promoters of *etoI*, *etoR*, *tolI* and *tolR* were fused to a promoterless *gfp* to perform a comparative *in vitro* transcriptional analysis of both systems in ET, ETETOI and ETTOLI genetic backgrounds. Results showed that *tolI* and *tolR* genes had considerably lower promoters activities in ET compared to the *etoI* and *etoR* promoters (Figure 2B). Additionally, transcription of *etoR* in ETTOLI was enhanced compared to ET and ETETOI, suggesting that the TolI/TolR system might repress *etoR* transcription. Taking into account the low activity of *tolI*/*tolR* promoters under the *in vitro* conditions used, we questioned if this system was activated *in planta*. To examine this possibility, co-inoculation of PSV with ET wild type harboring *tolI* promoter fused to GFP were carried out in micropropagated olive plants. No GFP fluorescence was detected for *tolI* promoter, whereas it was observed in the *etoI* promoter fusion, thus demonstrating that *tolI* gene expression was very low also *in planta*. We then decided to perform a comparative analysis by RT-qPCR of the transcription of *tolI* and *tolR* genes in two different media: the King's B rich medium and the Hrp-inducing medium which mimics the plant apoplast (27). Results of this experiment revealed a repression of both genes in the Hrp-inducing medium compared to King's B (Figure S1), which suggests that the environment of the plant might repress *tolI* and *tolR* transcription. It was therefore concluded that the TolI/R system was functional however it was repressed and/or not activated in ET under laboratory and *in planta* conditions that we have used. It cannot also be excluded that this AHL QS system is functional at very low AHL concentrations.

**Identification of the PSV NCPPB 3335 quorum sensing regulon**

It was of interest to establish the loci regulated by the PssI/R system thus a whole-genome transcriptional RNAseq comparative analysis of wild type PSV NCPPB 3335 and its derivative *pssI* mutant was performed. RNA was extracted from these strains grown in biological triplicates in LB broth to late-log phase and then sequenced as described in Material and Methods section. The results yielded a surprisingly small number of differentially expressed genes (DEGs) between the two strains (Table 5). To evaluate the reliability of the RNAseq results, the expression of these genes was analysed by RT-qPCR. Significant upregulation in the Δ*pssI* mutant was found only for three genes which encoded for PssR (PSA3335_1621), a pyruvate dehydrogenase E1 component beta subunit (PSA3335_1622, *pdhT*) and a pyruvate dehydrogenase E1 component (PSA3335_1624, *pdhQ*) (Table 5). On the other hand, downregulation of any of the genes identified by RNAseq analysis was not observed by RT-qPCR (Table 5). In conclusion, after combination of the results obtained by RNAseq and RT-qPCR, the *pssI* regulon of PSV NCPPB 3335 was restricted to only three genes (*pssR*, *pdhT* and *pdhQ*) under the conditions tested. The *pdhT* and *pdhQ* genes were also reported to be under the control of the *pssR* homolog in *P. syringae* pv. *syringae* (PSS) strain B728a (28). Interestingly, in PSS, a regulon study also resulted in very small number of genes regulated by AHL QS which are the same loci also determined to be regulated in PSV in this study (28).

**Identification of the ET DAPP-PG 735 quorum sensing regulon**

It was also of interest to determine the AHL QS regulon in ET therefore transcriptional profiling was also performed via RNAseq comparing the wild type against the ETETOI mutant as described in the Materials and Methods section. DEGs of significance ($p \leq 0.05$) were selected and listed in Table S2. In total, 308 DEGs were identified in the AHL synthase mutant ETETOI mutant, among which 162 loci were down-regulated and 146 up-regulated.

Interestingly, 19% of DEGs (59 genes) were classified as carbohydrate metabolism (Table 6) and, among them, 18 loci of inositol catabolism, which were negatively regulated by EtoI/R. On the other hand, DEGs involved in D-galactarate, D-glucarate and D-glycerate catabolism as well as maltose and maltodextrin utilization were positively regulated by the EtoI/R system. Besides carbohydrate metabolism, EtoI/R regulated genes mostly involved in the metabolism of amino acids, loci involved in membrane transport and in respiration. Furthermore, it was established that menaquinone and phylloquinone biosynthesis, glycerolipid and glycerophospholipid metabolism were influenced by EtoI/R. In addition, 9 transcriptional regulators belonging to the DeoR, IclR, LacI and TetR families were regulated by EtoI/R QS system.

In order to corroborate RNAseq results, nine QS-regulated genes were randomly selected and RT-qPCR was carried out with gene-specific primers (Table 3). RNA samples extracted from three biological replicate sets were used as templates for RT-qPCR. Expression patterns determined from RT-qPCR were in good accordance with the expression levels obtained by RNAseq (Figure 3).

**Role of PssI/R of PSV NCPPB 3335 *in planta***

In order to determine the role of the AHL QS system of PSV NCPPB 335 in virulence, the *ΔpssI* and *ΔpssR* mutants and their respective complemented strains were inoculated in micropropagated and in woody olive plants. In our conditions, no significant differences in knot development among the strains tested were found either in non-woody (micropropagated) or woody olive plants (Figure 3). Additionally, all bacteria reached a similar final population within the knots. It was concluded that PSV NCPPB 3335 AHL QS did not play a significant role in virulence under the conditions tested.

***In planta* role of QS regulated loci of *ET***

In order to study the possible role of some ET AHL QS regulated loci in the cooperative interaction with PSV, knock-out mutants in *iolD*, *iotS*, *garL*, *malK*, *gldA* and *hslV* genes were generated by insertion mutagenesis and co-inoculated with PSV in olive plants. Four of these DEGs (*iolD*, *iotS*, *garL* and *malK*) are involved in carbohydrate metabolism, which is the most representative category regulated by AHL QS in ET (see above). The *gldA* and *hslV*, on the other hand, encode for a glycerol dehydrogenase and ATP-dependent protease.

As previously established, co-inoculation of PSV with ET significantly increased the size of the olive knot (15, 16). When ET mutants, ETIOTS, ETMALK, ETGLDA and

ETHSLV were co-inoculated with PSV, olive knot size did not show any significant size alteration when compared when co-inoculated with ET wildtype (Figure 4A). Co-inoculation of PSV with ETGARL and ETIOLD, on the other hand, had a significant effect on the olive knot size with approximately a 50% reduction for ETGARL and approximately 20% increase for ETIOLD (Figure 4A). When co-inoculated with ETGARL, the colony forming units (CFU) of PSV in the knot were significantly reduced and resulted in 20% the amount of cells when co-inoculation was performed with the wildtype ET (Figure 4B). A significant reduction in the CFUs of PSV was also observed when co-inoculated with ETIOTS, ETGLDA and ETHSLV regardless that olive-knot size was not significantly affected. In order to further determine the putative role of GarL in PSV-ET interaction, we co-inoculated GFP-labeled PSV with ET wild type or the *garL* mutant constitutively expressing RFP. At 30 dpi knots were visualized in a stereoscopic microscope using GFP and RFP filters (Figure 5A, 5B) and pictures were taken and processed as described in Materials and Methods. Results show that the percentage of PSV population co-localization with ET wild type is under 5%, whereas over 75% of ET co-localize with PSV (Figure 5C). On the other hand, mutation in the ET *garL* gene resulted in a drastic reduction of ET association with PSV, with only 6.6% of the total ET population overlapping PSV. This result, together with the reduced knot size in PSV-ETGARL co-inoculation, indicated that GarL plays a major role in PSV-ET interaction.

## DISCUSSION

There is a growing need to study interspecies bacterial interactions since it is now becoming evident that most bacteria in the wild live as part of complex communities. Moreover in relation to diseases, reports are beginning to demonstrate that pathogens undergo interactions and communicate with non-pathogenic commensal/resident host microbial flora (11, 29). We have previously reported that the olive knot disease is a model to study interspecies communication and cooperation between a bacterial pathogen and commensal bacteria in a plant disease (14, 15). This cross-communication occurs via cross-feeding/sharing of AHL QS signals whereas the mechanism(s) of cooperation leading to a more aggressive disease is currently not understood and could be due to metabolite(s) sharing and/or metabolic complementarity. In this study, we determined the QS regulons of PSV and ET in order to begin to shed some light in this cooperative interspecies interaction in a plant disease.

Results presented here reveal that all *P. savastanoi* isolates infecting woody plants sequenced so far, harbor an identical content of AHL QS-related genes which consist of an archetypical AHL QS pair designated as *pssI*/*pssR*, and two *luxR* solos. The PssI/R system was firstly reported in strain DAPP-PG 722 (15) and displays 100% identity with PssI/R of strain NCPPB 3335 (studied here). At transcriptional level there is no QS positive feedback loop regulating the AHL synthase gene in PSV NCPPB 3335 (Figure 2A), which is contrast with what occurs in *P. syringae* pv *syringae* (PSS) B728a [50], a strain closely related with PSV from a phylogenetic point of view. It cannot be excluded that one of the two LuxR solos present in PSV genomes might be involved in *pssI* regulation. Moreover, AefR (AHL epiphytic fitness Regulator) positively regulates the *pssI* homolog *ahlI*, in *P. syringae* pv *phaseolicola* NPS3121 (30) and PSS B728a (31); a homolog of AefR is present in PSV genomes and could therefore have a similar function in regulating *pssI* in PSV.

*In planta* infection studies revealed that in PSV NCPPB 3335 neither *pssI* nor *pssR* are involved in virulence in the olive plant. It cannot be excluded however that AHL QS in PSV might plays a role in the epiphytic fitness/lifestyle *in planta*; QS has been shown to play a role in epiphytic fitness in PSS as well as other plant-associated bacteria (28, 31-33).

We found that wild type PSV NCPPB 3335 produces exclusively C6-AHL, whereas PSV DAPP-PG 722 synthesizes 3-oxo-C6- and 3-oxo-C8-AHLs (15) regardless that the *luxI* homologs are 100% identical; some other factor(s) might be responsible for the generation of different signal molecules. Overexpression of *pssI* in PSV NCPPB 3335 yielded 3-oxo-C6- and 3-oxo-C8-HSLs in addition to C6-AHL (Table 2), suggesting that different expression levels between these two strains might explain differences in AHL production. AHLs are synthesized by LuxI using *S*-adenosylmethionine and an acyl group which is provided by an acyl-carrier protein (ACP) (34). We have identified an ACP-encoding gene in the genome of PSV DAPP-PG 722 (locus tag GS14_RS0122650) which is not present in the PSV NCBBP 3335 genome; this locus might be involved in AHL synthesis and consequently lead to a dissimilar AHL profile synthesis between these two PSV strains. We previously reported 3-oxo-C6- and 3-oxo-C8-AHL production by ET DAPP-PG 735 (15) and here we demonstrated the production of four additional types of AHL (C6-, C8-, 3-oxo-C10- and 3-OH-C6-AHLs) using a more sensitive technique. The ability to produce more AHL types by ET increases its ability to crosstalk with bacterial neighbours. The PSV NCPPB 3335 can synthesize three out of the six types of AHL produced by ET indicating possible eavesdropping between PSV and ET via these AHLs. This is in line with our previous study which demonstrated rescue of the PSV QS response of a *pssI* mutant by co-inoculation with ET wild type (15).

This study reports the genetic loci regulated by AHL QS in a woody host pathogen of the *P. syringae* complex. Previous reports involve the two *P. syringae* herbaceous pathogens *P. syringae* pv *syringae* (PSS) and *P. syringae* pv. *tabaci* (PST). PSV NCPPB 3335 AHL QS regulon consists of only three genetically close loci, namely *pdhT, pdhQ* and *pssR*. In PSS strain B728a AHL QS regulates the transcription of only a 9 gene cluster located adjacent to the *ahlR-ahlI* locus which also contains the *pdhT* and *pdhQ* loci (28), whereas in PST strain 11528 over 300 genes were found to be regulated by QS, including *phdT, pdhQ* and the *pssR* homologs (35). Despite such a difference in AHL QS regulons among these strains, the transcription of *pdhT, pdhQ* and *pssR (ahlR)* is common in all *P. syringae* species and their role in *P. syringae* deserves further attention. (36).

QS in *Erwinia* species plays important roles in virulence determinants and secondary metabolite production (37). *E. toletana* is a harmless epiphyte and endophyte and was first isolated from olive knots caused by PSV, and is now a model to study multispecies interactions with PSV (14). ET DAPP-PG 735 possesses two canonical AHL QS systems, designated as EtoI/R and TolI/R. Prior to the availability of the genome sequence, AHL QS signals produced by ET were initially only attributed to EtoI (15). Here we report that promoter activities of *tolI/R* in ET, ETTOLI and ETETOI were very low and were barely detectable *in planta* and were found to be repressed by the plant apoplast mimic medium, suggesting that *tolI/R* is stringently regulated and might need a yet unidentified stimulus to be expressed. It is common that two or more AHL QS systems coexist in one bacterium and many of these are interconnected in their regulation (38-43). The uniqueness in *E. toletana* is that one system is stringently regulated probably requiring, in addition to cell-density, an environmental stimulus in order to be activated and/or de-repressed.

In ET, 308 genes were found to be regulated by EtoI/R controlling diverse functions such as membrane transport, protein metabolism, respiration, stress response, cell division and cell cycle. Interestingly, 59 loci were involved in metabolism of carbohydrates including inositol, D-galactarate, D-glucarate, maltose and maltodextrin indicating that it plays an important role in carbon resource acquisition. It was therefore of interest to study whether any of these carbohydrate metabolic pathways play a role in interspecies interactions and cooperation with PSV. As shown in Figure 4, when co-inoculated with several ET mutants in these pathways, PSV reached lower population densities, indicating that *iotS*, *garL*, *gldA* and *gslV* ET genes play a role in PSV-ET cross-communication. IN addition, co-inoculation of the ET *garL* mutant with PSV resulted in a significantly smaller olive knot. The alpha-dehydro-beta-deoxy-D-glucarate aldolase GarL catalyzes the cleavage of both 5-keto-4-deoxy-D-glucarate and 2-keto-3-deoxy-D-glucarate to pyruvate and tartronic semialdehyde (44). GarL is involved in D-galactarate, D-glucarate and D-glycerate catabolism synthesizing D-glycerate from galactarate. This demonstrates that ET-PSV cross-communication also occurs through some reactions of primary metabolism that not only affect the growth of PSV *in planta*, but also its virulence.

Applied and Environmental Microbiology

In summary, this work further demonstrated the role of AHL QS in the olive knot as well as metabolic interaction. This therefore further highlights the olive knot as a good model to study bacterial interspecies interactions in planta of a plant disease.

## MATERIALS AND METHODS

### Bacterial strains, media, growth conditions and recombinant DNA techniques

Bacterial strains used in this study are listed in Table 1. PSV and ET were grown at 28 °C and *Escherichia coli* was grown at 37 °C in Luria-Bertani (LB) medium (45) and Super Optimal Broth (SOB) (46). Solid and liquid media were amended when required with the appropriate antibiotic. Antibiotic concentration used were: kanamycin (Km) 10 µg ml$^{-1}$ for PSV and 50 µg ml$^{-1}$ for *E. coli*, gentamycin (Gm) 10 µg ml$^{-1}$, ampicillin (Ap) 400 µg ml$^{-1}$ for PSV and 100 µg ml$^{-1}$ for *E. coli*; and tetracycline 10 µg ml$^{-1}$.

All recombinant DNA techniques including restriction digestion, and agarose gel electrophoresis, purification of DNA fragments and ligations with T4 DNA ligase were performed as previously described (47). Plasmids were purified by using EuroGold columns (EuroClone, Italy) and were sequenced by Macrogen Europe (Amsterdam, NL) when necessary.

### Construction of bacterial strains

Plasmids and oligonucleotides used in this study are listed in Tables 2 and 3, respectively. PSV NCPPB 3335 *pssI* (PSA3335_1620) and *pssR* (PSA3335_1621) mutants were generated by allelic interchange. DNA fragments of approximately 1 kb corresponding to the upstream and downstream flanking regions of the gene to be deleted were amplified in three rounds of polymerase chain reaction (PCR) using Expand High Fidelity polymerase (Roche Applied Science, Mannheim, Germany). Restriction sites for *Hind*III were included in the primers as previously described (48). The resulting products, consisting on upstream and downstream flanking regions separated by the *Hind*III restriction site, were cloned into pGEMT-Easy (Promega, Madison, WI, U.S.A.) and sequenced to discard mutations. Next, the kanamycin resistance gene *nptII* was extracted by enzyme restriction from pGEMT-KmFRT- *Hind*III (49) and cloned in the plasmids mentioned above to generate pECP10-Km and pECP11-Km (Table 2). All the plasmids generated for the construction of PSV NCPPB 3335 mutants were suicide vectors in PSV. Plasmids were transferred to NCPPB 3335 by electroporation (17) and transformants were selected in LB-Km plates. To select the allelic interchange (double recombination event) and discard plasmid integration (single recombination event), individual colonies were replicated into LB-Ap plates and $Ap^R$ colonies were discarded. Southern blot analyses were carried out to confirm single integration in the correct position in PSV genome.

Mutation of selected genes in ET was performed via a single homologous recombination event with the use of pKNOCK-Km suicide delivery system as previously described (50) generating mutants of ETIOLD, ETIOTS, ETGARL, ETMALK, ETGLDA, ETHSLV, ETTOLI and ETTOLR. Briefly, internal fragments from *iolD* (G200_RS0103425), *iotS* (G200_RS0119945), *garL* (G200_RS0124305), *malK* (G200_RS0114460), *gldA* (G200_RS0114990), *hslV* (G200_RS0113655), *tolI* (G200_RS0118785) and *tolR* (G200_RS0118780) of ET were amplified using the primers listed in Table 3 and cloned in conjugative suicide vector pKNOCK-Km. The generated plasmids having internal fragments from selected genes were transformed into *E. coli* S17-1 λpir and delivered to ET for its homologous recombination. $Km^R$ colonies were verified by PCR analysis followed by sequencing of the targeted gene to confirm the generation of ET mutants.

**AHL extraction and characterization**

Bacterial strains were grown overnight in LB broth (final volume 100 ml); cells were then removed by centrifugation and the supernatant was used to purify AHLs. Spent supernatants were filtered (pore diameter 0.45 µm), mixed with one volume of 0.1% acetic acid (v/v) in ethyl acetate and incubated under shaking conditions for 30 minutes. The organic phases were dried at room temperature. The AHLs produced by each strain were identified from the organic extracts of spent supernatants by liquid chromatography-electrospray ionization-tandem mass spectrometry (LC-ESI-MS/MS) as we described previously (51). As an example of this analysis, the ion chromatograms of an AHL standard and the *E. toletana* wild type sample is provided in Figure S3.

**Construction of plasmids and reporter assays**

For the complementation of PSV Δ*pssI* and Δ*pssR* mutant strains, the entire open reading frames of each gene and their corresponding promoter and transcriptional terminator regions were amplified by PCR using Expand High Fidelity polymerase (Roche Applied Science, Mannheim, Germany) and cloned into pGEMT-Easy (Promega, Madison, WI, USA). After sequencing to discard mutations, the fragments were directionally subcloned into pBBR:MCS5 yielding pBBR:*pssI* and pBBR:*pssR*.

DNA fragments of 338 and 352 bp containing *pssI* and *pssR* promoter regions, respectively, were amplified by PCR using oligonucleotides listed in Table 3 and cloned into pMP220 (52). The resulting plasmid *lacZ* transcriptional fusions were transferred to PSV by electroporation and β-galactosidase activity was measured as described previously (45). Bacteria were grown in LB broth amended with 10 µg $ml^{-1}$ tetracycline at an initial $OD_{600nm}$ of 0.3 and β-galactosidase activity was measured throughout the growth curve.

Promoter regions of *etoI*, *etoR*, *tolI* and *tolR* ET genes were amplified by PCR using the oligonucleotides listed in Table 3 and cloned in the vector pBBR:GFP (53) in order to be transcriptionally fused to a promoterless *gfp* gene. The resulting plasmids were transformed by electroporation into ET strains (54) and gene promoter activity was determined as the amount of GFP fluorescence measured in the late log phase at 510nm on a microplate reader (Perkin Elmer EnVision 2104). The expression of *tolI* and *tolR* was also analyzed by RT-qPCR in King's B and Hrp-inducing medium as reported previously (48). The *etoI* and *tolI* promoter activities were measured *in vivo* in mixed PSV-ET infections. Ten plants were inoculated with each of the three combinations: PSV and ET expressing a promoterless GFP (negative control), PSV and ET-pBBR:$P_{etoI}$-GFP, and PSV and ET-pBBR:$P_{tolI}$-GFP. The presence/absence of fluorescence was verified using a stereoscopic microscope (Leica MZ FLIII; Leica Microsystems, Wetzlar, Germany).

**RNA extraction, RNAseq and analysis**

Ribopure bacteria RNA isolation kit (Ambion Inc., Austin, TX, U.S.A.) was used for total RNA extraction from three biological replications. Bacteria were grown in LB until the onset of stationary phase and about 2 x $10^9$ cells were collected for RNA extraction following the manufacturer's instructions. Library preparation and transcriptome sequencing were performed by IGA Technology Services Srl (Udine, Italy). Briefly, libraries were constructed with TruSeq Stranded mRNA Sample Prep kit (Illumina, San Diego, CA) and single-end sequencing was carried out on HiSeq2500 (Illumina, San Diego, CA). Illumina adapters, lower quality bases and poly-A tails were removed using ERNE (55). Software and tools for *de novo* assembly and comparisons were performed as previously described (56-58). The false discovery rate (FDR) with a significance level of ≤0.05 and with a minimum fold change set as the threshold were used to judge the significance of gene expression difference. Reads obtained from adapter removal were aligned against GCA_000336255.1 and GCA_000164015.2 reference genome assemblies. Features counts produced by RNA-seq were normalized and analyzed with DeSeq2 software (http://dx.doi.org/10.1186/s13059-014-0550-8) to calculate differential expression values ($log_2$ of the fold change LFC) and raw p-values. To select differentially expressed genes, genes raw p-values were corrected for multiple testing using with the false discovery rate (FDR) method (59). Final selection was based on genes with FDR ≤0.05. The original RNAseq data has been submitted in the Sequence Read Archive (SRA) as submission number SUB3743389

**Validation of RNAseq data using qRT-PCR**

Quantitative real-time PCR was performed on CFX96 Touch qPCR system (Bio-Rad, Hercules, CA, USA) to validate expression patterns from transcriptome analysis. cDNA was generated following the manufacturer's protocol of Reverse Transcription system kit (Promega, Madison, WI, USA) starting with 1-2 µg of purified RNA as input. Diluted with RNase-free water, the synthesized cDNA samples were adjusted to 25 ng·$\mu L^{-1}$ and were measured by Nano Drop 2000 (Thermo scientific, Wilmington, DA, USA). In each reaction, 2 µL of cDNA template was mixed with GoTaq qPCR Master Mix kit (Promega, Madison, WI, USA) and specific primers (Table 3) to a final volume of 12 µl. qPCR primer designing was performed with free online software following the instructions of Brenda Thornton and Chandak Basu (60). Each reaction was carried out initially with 2 min at 95 °C, followed by 45 cycles of PCR (95 °C, 15 s; 60 °C, 30 s). The relative transcript abundance was calculated using the cycle threshold (ΔΔCt) method (61). Transcriptional data were normalized to the *gyrA* (for PSV) or *recA* (for ET) housekeeping genes.

***In planta* experiments**

Olive plants were micropropagated and inoculated as detailed previously (62). Briefly, micropropagated olive plants were wounded by excision of an intermediate leaf and infected in the stem wound with a bacterial suspension under sterile conditions. For this purpose, bacterial lawns were grown for 48h on LB plates, washed twice with 10 mM $MgCl_2$ and resuspended in 10 mM $MgCl_2$ to an approximate concentration of $10^8$ CFU·$mL^{-1}$. Suspension of PSV alone or mixed with ETIOLD, ETIOTS, ETGARL, ETMALK, ETGLDA and ETHSLV respectively in 1:1 (vol:vol) ratio were prepared. Plants were inoculated with approximately $5x10^3$ total CFU and kept in a growth chamber for 30 days, as previously described (62). The morphology of the knots was observed with a stereoscopic microscope 30 days post-inoculation (dpi) (Leica MZ FLIII; Leica Microsystems, Wetzlar, Germany), also equipped with a 100 W mercury lamp, a GFP2 filter (excitation 480/40 nm; emission 510LP nm) and a red fluorescent protein (RFP) filter (excitation 546/10 nm; emission 570LP nm). For the quantification of green (GFP-tagged PSV) and red (RFP-tagged ET and ETGARL strains) pixels, two pictures per knot (corresponding to the front and back sides of the tumour) were taken with each the GFP2 and RFP filters. Pictures were transformed to 8-bits images and overlapped with Fiji ImageJ (https://imagej.net/Fiji) using the Image correlator plugin. The number of green pixels overlapping red pixels, indicating the population of PSV that co-localize with ET/ETGARL, was determined for both the front and the back sides of each knot and an average per knot was calculated. An identical procedure was used to determine the percentage of ET or ETGARL population that co-localize with PSV. Bacteria were recovered from the knots using a mortar and pestle containing sterile $MgCl_2$ 10 mM. Serial dilutions were plated on LB plates supplemented with the corresponding antibiotic when required. Knots were 3D scanned and the knot size determined using the Neftabb Basic 5.2 software.

The virulence of PSV and its derived mutants and complemented strains was also analysed on 1-year old olive plants on 1-year old olive plants (*Olea europaea*) derived from a seed originally collected from a cv. Arbequina plant as detailed before (17, 63, 64). Morphological changes scored at 90 dpi were captured with a high-resolution camera Canon D6200 (Canon Corporation, Tokyo, Japan). The knot volume was calculated from a minimum of three representative knots as described previously (15, 65).

**Acknowledgements**

ECP acknowledges the contribution of an EMBO fellowship, MX of a Chinese Scholarship Council fellowship whereas DPD and GU of an ICGEB fellowship.

**Figure Legends**

**Figure 1**. Gene arrangement of quorum sensing system elements in the genomes of PSV NCPPB 3335 and ET DAPP-PG 735. (A) *pssI* and *pssR* represent a canonical *luxI*/*luxR* gene pair, whereas *luxR2* and *luxR3* correspond to orphan *luxR* homologs in PSV NCPPB 3335. (B) *etoI/etoR* and *tolI*/*tolR* represent two canonical *luxI*/*luxR* gene pairs of ET DAPP-PG 735. Codes above arrows correspond to locus tags

**Figure 2**. Promoter activities of PSV and ET quorum sensing genes. (A) β-galactosidase activity of *pssI* promoter fusion to *lacZ* measured in PSV NCPPB 3335, Δ*pssI* and Δ*pssR* at log (4 hours incubation) and stationary phase (10 hours incubation). PSV harboring a promoterless *lacZ* (empty pMP220 plasmid) was included as a control. Asterisks indicate a significant difference (student's *t* test, $P < 0.05$) in promoter activity in stationary phase compared to log phase (B) GFP fluorescence of *etoI*, *etoR tolI* and *tolR* fusions to *gfp* measured in ET, ETTOLI and ETETOI backgrounds. GFP fluorescence was normalized to $OD_{600}$. Bars represent the average of three independent replications ± the standard deviation

**Figure 3**. Evaluation of RNAseq-based expression patterns of ET using RT-qPCR. The expression patterns of randomly selected genes were analyzed by RT-qPCR to validate RNAseq results. The values of fold difference were average of three biological replicates which were calculated by using comparative quantification method. $Log_2$ ratio of obtained values was compared with $log_2$ ratio of (ETETOI/ET) FPKM values.

**Figure 4**. Role of ET AHL QS loci in the PSV-ET cooperation *in planta*. (A) Size of the knots induced in micropropagated olive plants at 30 dpi by PSV in combination with ET

strains. (B) CFU of PSV and (C) CFU of ET recovered from knots. Bars indicate the average of, at least, three knots ± standard deviation.

**Figure 5**. Knots developed at 30 dpi in micropropagated olive plants after co-inoculation of GFP-labelled PSV with RFP-labelled ET or ETGARL. (A) Co-inoculation using GFP-labelled PSV and RFP-labelled ET. (B) Co-inoculation using GFP-labelled PSV and RFP-labelled ETGARL. (C) Percentage of the PSV and ET/ETGARL populations co-localization within the knot. Bars represent the average of six independent knots ± standard deviation.

**Table 1.** Bacterial strains used in this study

| Bacterial Strains | Relevant characteristics | Source |
|---|---|---|
| *Escherichia coli* | | |
| DH5α | F– Φ80*lac*ZΔM15 Δ(*lac*ZYA-*arg*F) U169 *rec*A1 *end*A1 *hsd*R17 (rK–, mK+) *pho*A *sup*E44 λ– *thi*-1 *gyr*A96 *rel*A1 | Invitrogen-LifeTechnologies |
| S17-1λpir | $Km^R$, recA, pro, hsdR, RP4-Tc::Mu-Km::Tn7, pir | (66) |
| *Erwinia toletana* | | |
| DAPP-PG 735 | Wild type | (15) |
| ETETOI | Deletion *etoI* mutant of ET DAPP-PG735 | (15) |
| ETETOR | Deletion *etoR* mutant of ET DAPP-PG735 | (15) |
| ETTOLI | Deletion *tolI* mutant of ET DAPP-PG735 | This study |
| ETTOLR | Deletion *tolR* mutant of ET DAPP-PG735 | This study |
| ETIOLD | Deletion *iolD* mutant of ET DAPP-PG735 | This study |
| ETIOTS | Deletion *iotS* mutant of ET DAPP-PG735 | This study |
| ETGARL | Deletion *garL* mutant of ET DAPP-PG735 | This study |
| ETMALK | Deletion *malK* mutant of ET DAPP-PG735 | This study |
| ETGLDA | Deletion *gldA* mutant of ET DAPP-PG735 | This study |
| ETHSLV | Deletion *hslV* mutant of ET DAPP-PG735 | This study |
| ETETOI-pBBR:*etoI* | ETETOI complemented with pBBR:*etoI* | This study |
| ETTOLI-pBBR:*tolI* | ETTOLI complemented with pBBR:*tolI* | This study |
| *Pseudomonas savastanoi* pv. *savastanoi* | | |
| NCPPB 3335 | Wild type | (17) |
| Δ*pssI* | Deletion *pssI* mutant of NCPPB 3335 ($Km^R$) | This study |
| Δ*pssR* | Deletion *pssR* mutant of NCPPB 3335 ($Km^R$) | This study |
| Δ*pssI*-pBBR:*pssI* | Δ*pssI* complemented with pBBR:*pssI* | This study |
| Δ*pssR*-pBBR:*pssR* | Δ*pssR* complemented with pBBR:*pssR* | This study |

**Table 2** Plasmids used in this study

| | | |
|---|---|---|
| pGEM-T Easy | Cloning vector; Amp$^R$ | Promega |
| pKNOCK-Km | Conjugative suicide vector; Km$^R$ | (50) |
| pKNOCK- IOLD | Internal PCR iolD fragment of ET DAPP-PG 735 cloned in pKNOCK-Km; Km$^R$ | This study |
| pKNOCK- IOTS | Internal PCR iotS fragment of ET DAPP-PG 735 cloned in pKNOCK-Km; Km$^R$ | This study |
| pKNOCK- GARL | Internal PCR garL fragment of ET DAPP-PG 735 cloned in pKNOCK-Km; Km$^R$ | This study |
| pKNOCK- MALK | Internal PCR malK fragment of ET DAPP-PG 735 cloned in pKNOCK-Km; Km$^R$ | This study |
| pKNOCK- GLDA | Internal PCR gldA fragment of ET DAPP-PG 735 cloned in pKNOCK-Km; Km$^R$ | This study |
| pKNOCK- HSLV | Internal PCR hslV fragment of ET DAPP-PG 735 cloned in pKNOCK-Km; Km$^R$ | This study |
| pECP10-Km | pGEM-T Easy derivative containing 1kb on each side of the *pssI* (PSA3335_1621) gene from NCPPB 3335 interrupted by the kanamycin resistance gene *nptII* (Ap$^R$, Km$^R$) | This study |
| pECP11-Km | pGEM-T Easy derivative containing 1kb on each side of the *pssR* (PSA3335_1622) gene from NCPPB 3335 interrupted by the kanamycin resistance gene *nptII* (Ap$^R$, Km$^R$) | This work |
| pGEMT-KmFRT-HindIII | Contains KmR from pKD4 and HindIII sites (ApR KmR) | This work |
| pBBR:*pssI* | pBBR1MCS-5-derivative containing the PSV NCPPB 3335 *pssI* and its promoter region (352 bp) flanked by *Eco*RI and *Xba*I restriction sites (Gm$^R$) | This work |
| pBBR:*pssR* | pBBR1MCS-5-derivative containing the PSV NCPPB 3335 *pssR* and its promoter region (435 bp) flanked by *Eco*RI and *Xba*I restriction sites (Gm$^R$) | This work |
| pMP220 | Promoter probe vector, IncP, LacZ; Tc$^R$ | (52) |
| pMP220-P*pssI* | Transcriptional fusion of PSV *pssI* promoter to *lacZ* | This work |
| pLRM1-GFP | Overexpression of GFP from pBBRMCS5 | (67) |
| pBBR:RFP | pBBRMSC5 containing RFP | (53) |
| pBBR:GFP | pBBRMSC5 containing a promoterless GFP | (53) |
| pBBR:P*etoI*-GFP | Transcriptional fusion of ET *etoI* promoter to GFP | This work |
| pBBR:P*etoR*-GFP | Transcriptional fusion of ET *etoR* promoter to GFP | This work |
| pBBR:P*tolI*-GFP | Transcriptional fusion of ET *tolI* promoter to GFP | This work |
| pBBR:P*tolR*-GFP | Transcriptional fusion of ET *tolR* promoter to GFP | This work |
| pBBR:*etoI* | pBBR1MSC-5 containing *etoI*, Described as pBBRToll in previous publication | (15) |
| pBBR:*tolI* | pBBR1MSC-5 containing *tolI* | This work |

**Table 3** Primers used for cloning purposes

| Primers used for cloning purposes | | |
|---|---|---|
| Plasmid | Primer name | Primer sequence |
| pKNOCK- IOLD | iolD_pnkFw | AGATCTCACCAGATTCCGTTTGCCG |
| | iolD_pnkRev | CTCGAGCTGTTGTAATCCCTGGTGCG |
| pKNOCK- IOTS | iotS_pnkFw | AGATCTGCTGACCGATAAAATGGCGT |
| | iotS_pnkRev | CTCGAGACCAATCGCCATTTCATCGT |
| pKNOCK- GARL | garL_pnkFw | AGATCTGTCCACCTTGCAACGAACC |
| | garL_pnkRev | CTCGAGGAGCTGGGTTTCGATTTGCA |
| pKNOCK- MALK | malK_pnkFw | AGATCTATTGGTCGCACGCTGGTC |
| | malK_pnkRev | CTCGAGCGATGGCCTTGTTAGTGACC |
| pKNOCK- GLDA | gldA_pnkFw | AGATCTCCGATGAAGGGGTGTTTGAA |
| | gldA_pnkRev | CTCGAGCCAGACCGCCATTCTCAAAG |
| pKNOCK- HSLV | hslV_pnkFw | AGATCTGGTCATCTGGTTAAAGCCGC |
| | hslV_pnkRev | CTCGAGCACCTGAACCGATGGCAATA |
| pKNOCK-tolI | muttolIFw | GGATCACTGTGCCCTTTA |
| | muttolIRev | TTATCCTCAGAGTGAATCAGCC |
| pKNOCK-tolR | muttolRFw | TACGCGACCTGAGACGCATC |
| | muttolRRev | ATTTTACGATTTCCAGCTCGCG |
| pBBR:P*tolI*-GFP | PtolIFw | CAGAGATCTCGCTGATTC |
| | PtolIRev | CGAATTCCGCCAACAACGA |
| pBBR:P*tolR*-GFP | PtolRFw | AATCGTGGATCCGCGG |
| | PtolRRev | CGAATTCACCACACCAG |
| pBBR:P*etoI*-GFP | PetoIFw | TTAGATCTAAATCACGTAACAAC |
| | PetoIRew | ATTCGAATTCATATCAAA |
| pBBR:P*etoR*-GFP | PetoRFw | CAGATCTGCTCTTCCTGTAATGGGA |
| | PetoIRew | CGAATTCACATTTGCCTGACCTCAA |
| pBBR:*pssI* | pssI_F-331 | TCTAGATCGCTCTGATCCTGATGAGTG |
| | pssI_R924 | GAATTCCTCATCCGCTTCCATGACC |
| pBBR:*pssR* | pssR-F-417 | TCTAGAAGACGCTCGACGATGTCG |
| | pssR_R993 | GAATTCTTGCAATCGATCATCACGG |
| pBBR:*tolI* | tolIFw | GTCTCGAGCAAATCTGCTGATGCCGC |
| | tolIRev | GGACTAGTGCCTGGCTGCTGATTACTTT |
| pMP220-P*pssI* | pssI_F-279 | ACTCATGGAGATCTGGCAGAGATTTCGTGTTGGG |
| | pssI_R35 | ACTCATGGGGTACCGTAACGGGCATCGTCGTG |
| pBBR:*pssI* | pssI_F-331 | TCTAGATCGCTCTGATCCTGATGAGTG |
| | pssI_R924 | GAATTCCTCATCCGCTTCCATGACC |
| pBBR:*pssR* | pssR-F-417 | TCTAGAAGACGCTCGACGATGTCG |
| | pssR_R993 | GAATTCTTGCAATCGATCATCACGG |
| Primers used for the construction of *pssI* and *pssR* mutants | | |
| *pssR* | PssR_F-1008 | CATTCCAGTGCTCCTTGAGC |
| | TAPssR_R3 | AAGCTTGACTCACTATAGGGGCTTTCACGGTACGA ACCTC |
| | TDPssR_R739 | CCCTATAGTGAGTCAAGCTTCCATCAACATGGGCAT GG |
| | PssI_F-332 | CCTGATGAGTGTGTGCATCG |
| *pssI* | TAPssI_R4 | CCCTATAGTGAGTCAAGCTTCATGCATAGCGCTGCC TG |
| | PssI_F-983 | GATATCGGCGTTGATGTCCTG |
| | TDPssI_F680 | CCCTATAGTGAGTCAAGCTTCATGCATAGCGCTGCC TG |
| | PssR_F-280 | TGCGCTGTTCATCACTACTCC |
| Primers used in the qPCR experiments | | |
| Gene ID | Gene function | Primer sequence |
| *E. toletana* genes | | |
| G200_RS0108970 | PTS lactose transporter subunit IIB | F: ACTCTGCGTATGTGGCTG<br>R: TCGCTGGCATCTGAGGTT |
| G200_RS0124540 | Recombinase RecA | F: CAGGCGATGCGTAAACTGG |

| | | |
|---|---|---|
| | | R: GGCGAACAGAGGCGTAGA |
| G200_RS0112020 | Sigma-fimbria uncharacterized paralogous subunit | F: CCTCGGTGTTGCCTCTTC<br>R: CCATTGCCTGCTGAACCC |
| G200_RS0112675 | SulP family transporter | F:GTGTATGTGGTGGCGGTG<br>R: CACTGAGGTAATCGGCAAGC |
| G200_RS0113655 | ATP-dependent protease HslV | F: GTAGTGATTGGCGGCGATG<br>R: CCACAGCGGCTTTAACCAG |
| G200_RS0114400 | Conjugal transfer protein TraF | F: GGCTACACCGATACTTACCAGA<br>R: CACGATAACCACCACGCAA |
| G200_RS0103275 | HlyD family secretion protein | F: AAACCCGCATCAACCCAC<br>R: ATCACGCTTCACCTCATCCT |
| G200_RS0103290 | Hemagglutinin | F: CCTGTTGCTGGGTTCATTGTT<br>R: GTGGTGGTAGCCGAGGTTT |
| G200_RS0123635 | Transcriptional regulator, TetR family | F: GCAGTCACAGGATGCGATTC<br>R: TGAGCCATACACCAGCGATAG |
| G200_RS0123645 | TIM-barrel signal transduction protein | F: CGCTGAAACCGCACTGAAA<br>R: GCCGTAGAAACCATCGCAAA |
| G200_RS0118785 | *tolI* | F: TGGAGAAGGCTGGTCTATTC<br>R: GCATTAAAGGGCACAGTGAT |
| G200_RS0118780 | *tolR* | F: TAATGCGTCTGAAACTGGTC<br>R: CGACATATTTCTTCTGCCGA |
| *P. savastanoi* pv. **savastanoi** genes | | |
| PSA3335_1622 | Pyruvate dehydrogenase E1 component, beta subunit | F: TCAAGGAGCACTGGAATGTCG<br>R: TCTTCAAGGGATGGAAACGATT |
| PSA3335_1624 | Pyruvate dehydrogenase E1 component | F: CGATACCGTGCTGTGTGTCT<br>R: GATCAGGGTGCGGGTAGTTC |
| PSA3335_1621 | LuxR transcriptional regulator | F: ACTGCCCACCGTTGAAGATAA<br>R: CATAAGATTTCAGCCAGGAGTCG |
| PSA3335_2315 | Putative hydrocarbon oxygenase | F: TGCCGTTCTTCCTGGCTTA<br>R: ACCCGTCATTCATCCACCG |
| PSA3335_4742 | Urocanate hydratase | F: AGCGGGCATTCCTACCTTC<br>R: AGAACAACGGGCGGATGTA |
| PSA3335_1620 | Homoserine lactone synthase | F: CACTGACCGAAATGCTGCTGT<br>R: TTGCTGACCACCGTGATGAT |
| PSA3335_4623 | Copper chaperone | F: GACTCAAGCGATCAAGAACGATG<br>R: CTGCTCGGGTGACAGACTG |
| PSA3335_2048 | Hypothetical protein | F: AATACCACCGCATCGACGAA<br>R: TCACGCCGTTGACCAGAAA |
| PSA3335_0454 | Malonate decarboxylase delta subunit | F: TTCGCCAGGCAAGCTATCAA<br>R: TCCTCGAAGCCCTGATCCA |
| PSA3335_2054 | Hypothetical protein | F: TGAGCATCTACAGGCTTCGGA<br>R:<br>CATGTTGATAAGGAATGAGGTTCG |
| PSA3335_4121 | Pectin lyase precursor | F: CCAAGGTGCAGGACTGTTCA<br>R: GATACGGGCGAAGGTGTTGT |

**Table 4**. Quantification of AHLs produced by PSV NCPPB 3335 and ET DAPP-PG 735[a]

| | C6-AHL | C8-AHL | 3-oxo-C6-AHL | 3-oxo-C8-AHL | 3-oxo-C10-AHL | 3-OH-C6-AHL |
|---|---|---|---|---|---|---|
| PSV | + | - | - | - | - | - |
| Δ*pssI* | - | - | - | - | - | - |
| Δ*pssI*-pBBR:*pssI* | +++ | + | +++ | ++ | - | - |
| ET | +++ | + | +++ | +++ | + | ++ |
| ETETOI | - | - | - | - | - | - |
| ETETOI-pBBR:*etoI* | +++ | +++ | +++ | +++ | +++ | +++ |
| ETTOLI | +++ | + | +++ | +++ | - | ++ |
| ETTOLI-pBBR:*tolI* | +++ | + | +++ | +++ | - | ++ |

[a] -, no production; +, relative peak area <100,000; ++, relative peak area between 100,000 and 1,000,000; +++, relative peak area >1,000,000

**Table 5.** Genes regulated by *pssI* in PSV NCPPB 3335

| Locus tag[a] | Gene[b] | Gene product | RNAseq[c] | RT-qPCR[c] |
|---|---|---|---|---|
| Upregulated | | | | |
| PSA3335_1622 | *pdhT* | Pyruvate dehydrogenase E1 component, beta subunit | 3.27 | 3.6 |
| PSA3335_1624 | *pdhQ* | Pyruvate dehydrogenase E1 component | 2.97 | 2.32 |
| PSA3335_1621 | *pssR* | LuxR transcriptional regulator | 1.44 | 3.95 |
| | | | | |
| Downregulated | | | | |
| PSA3335_4623 | UN | Copper chaperone | -1.07 | -0.82 |
| PSA3335_4121 | UN | Pectin lyase precursor | -0.92 | 0.52 |

[a]Upregulated or downregulated genes in the Δ*pssI* mutant according to RNAseq data.
[b]UN, unnamed
[c]The $\log_2$ (fold change) obtained in the RNAseq and RT-qPCR experiments are represented. The fold change refers to the ratio of the average expression obtained in the Δ*pssI* mutant versus the wild type strain in three biological replicates. Genes which QS-dependent expression was corroborated by RT-qPCR are underlined

**Table 6**. Genes regulated by *etoI* in ET DAPP-PG 735 classified as carbohydrates metabolism

| Gene ID | $log_2$(ETEOI/ET) | FDR | Gene product |
|---|---|---|---|
| Inositol catabolism | | | |
| G200_RS0101695 | 2.56366058 | 1.13E-09 | Major myo-inositol transporter IolT |
| G200_RS0103410 | 2.81622077 | 3.38E-45 | Inosose dehydratase IolE |
| G200_RS0103415 | 3.051765216 | 2.74E-47 | Glyceraldehyde-3-phosphate ketol-isomerase IolH |
| G200_RS0103420 | 3.612129551 | 3.41E-57 | Myo-inositol 2-dehydrogenase 1 IolG |
| G200_RS0103425 | 3.034782963 | 1.24E-11 | Epi-inositol hydrolase IolD |
| G200_RS0103430 | 2.455264684 | 4.22E-08 | 5-keto-2-deoxygluconokinase IolC |
| G200_RS0103435 | 1.82595615 | 7.10E-18 | Transcriptional regulator of the myo-inositol catabolic operon IolR |
| G200_RS0103440 | 2.322930823 | 6.16E-29 | 5-deoxy-glucuronate isomerase IolB |
| G200_RS0103445 | 2.343048715 | 1.92E-08 | Methylmalonate-semialdehyde dehydrogenase IolA |
| G200_RS0103450 | 2.393433177 | 3.58E-08 | Inosose isomerase IolI |
| G200_RS0103485 | 2.265947451 | 7.57E-22 | Inosose dehydratase |
| G200_RS0103490 | 1.606575527 | 5.42E-13 | Myo-inositol 2-dehydrogenase |
| G200_RS0109945 | 2.054104613 | 1.56E-06 | Myo-inositol 2-dehydrogenase |
| G200_RS0111735 | 2.826752946 | 1.30E-21 | Major myo-inositol transporter IolT |
| G200_RS0119935 | 2.36064358 | 6.17E-31 | Inositol transport system permease protein |
| G200_RS0119940 | 2.922693363 | 5.94E-43 | Inositol transport system ATP-binding protein |
| G200_RS0119945 | 2.723773939 | 6.09E-34 | Inositol transport system sugar-binding protein |
| G200_RS0120045 | 2.507147476 | 1.44E-09 | Myo-inositol 2-dehydrogenase 2 |
| D-galactarate, D-glucarate and D-glycerate catabolism | | | |
| G200_RS0114355 | -1.471923639 | 1.25E-06 | MFS transporter |
| G200_RS0124280 | -2.146858379 | 7.57E-39 | D-galactarate dehydratase GarD |
| G200_RS0124290 | -2.155286292 | 3.22E-65 | D-glucarate permease |
| G200_RS0124295 | -1.762097381 | 2.90E-22 | Glucarate dehydratase GudD |
| G200_RS0124300 | -1.801096855 | 3.95E-16 | Glucarate dehydratase GudD |
| G200_RS0124305 | -1.841655614 | 7.57E-39 | 2-dehydro-3-deoxyglucarate aldolase GarL |
| G200_RS0124320 | -1.921850417 | 2.06E-49 | Glycerate kinase |
| G200_RS25820 | -2.073060541 | 9.97E-53 | 3-hydroxyisobutyrate dehydrogenase GarR |
| Maltose and Maltodextrin catabolism | | | |
| G200_RS0105520 | -1.474187006 | 1.51E-22 | PTS system, maltose and glucose-specific IIABC component |
| G200_RS0114455 | -2.146215061 | 6.10E-08 | Maltose/maltodextrin high-affinity receptor LamB |
| G200_RS0114460 | -3.460976388 | 1.17E-46 | Maltose/maltodextrin transport ATP-binding protein MalK |

| | | | |
|---|---|---|---|
| G200_RS0114465 | -3.432632153 | 3.66E-74 | Maltose/maltodextrin ABC transporter, substrate binding periplasmic protein MalE |
| G200_RS0114470 | -1.356395147 | 1.92E-06 | Maltose ABC transporter permease MalF |
| Other carbohydrates metabolism | | | |
| G200_RS0102345 | -1.326068817 | 1.39E-19 | 6-phospho-beta-glucosidase |
| G200_RS0120860 | -1.385897754 | 2.78E-07 | PTS beta-glucoside transporter subunit EIIBCA |
| G200_RS0109880 | 1.195365256 | 3.02E-14 | Beta-glucuronidase |
| G200_RS0108005 | 1.553737025 | 2.47E-29 | Alcohol dehydrogenase |
| G200_RS0118365 | 1.430810069 | 6.79E-14 | Pyruvate formate-lyase |
| G200_RS0108900 | 1.148093171 | 1.24E-10 | Deoxyribose-phosphate aldolase |
| G200_RS0116155 | 1.055489576 | 4.73E-12 | Ribokinase |
| G200_RS0109855 | 1.1278524 | 1.96E-13 | Mannonate dehydratase |
| G200_RS0102390 | 2.327906926 | 3.00E-11 | Gluconate 2-dehydrogenase, membrane-bound, flavoprotein |
| G200_RS0102395 | 2.004607764 | 1.22E-17 | Gluconate 2-dehydrogenase, membrane-bound, gamma subunit |
| G200_RS0119505 | 1.507781586 | 2.74E-15 | Ribose ABC transport system, periplasmic ribose-binding protein RbsB |
| G200_RS0118360 | 1.344548034 | 3.43E-28 | Pyruvate formate lyase 1-activating protein PflA |
| G200_RS0121040 | 1.68097694 | 2.43E-04 | Aerobic glycerol-3-phosphate dehydrogenase GlpD |
| G200_RS0121025 | -1.369452767 | 7.02E-22 | Glucose-1-phosphate adenylyltransferase GlgC |
| G200_RS0121030 | -1.413808857 | 4.42E-26 | Glycogen synthase GlgA |
| G200_RS0108965 | 1.651181716 | 2.59E-16 | 6-phosphofructokinase |
| G200_RS0105430 | -1.010271981 | 3.98E-16 | Aconitate hydratase AcnA |
| G200_RS0114595 | -1.302381077 | 1.85E-17 | Malate synthase |
| G200_RS0101545 | -2.502124169 | 2.13E-42 | L-lactate dehydrogenase |
| G200_RS0109845 | 1.012221802 | 6.78E-09 | MFS transporter LacY |
| G200_RS0118000 | 1.499549769 | 9.33E-05 | 6-phosphogluconolactonase |
| G200_RS0100900 | -1.050323621 | 2.49E-14 | DUF485 domain-containing protein |
| G200_RS0100905 | -1.143638292 | 2.68E-11 | Cation/acetate symporter ActP |
| G200_RS0121020 | -1.529478972 | 2.20E-39 | Glycogen debranching enzyme |
| G200_RS0113990 | 1.292475653 | 5.30E-11 | PTS sugar transporter subunit IIB |
| G200_RS0113995 | 1.209666009 | 1.43E-15 | Putative carbohydrate PTS system, IIA component |
| G200_RS0114000 | 1.458640254 | 1.69E-13 | Putative transcriptional regulator of unknown carbohydrate utilization cluster, GntR family |
| G200_RS0104280 | -1.044495518 | 3.39E-06 | Alpha/beta hydrolase |

| **Gene ID** | **$log_2$(ETEOI/ET)** | **FDR** | **Gene product** |
|---|---|---|---|
| Inositol catabolism | | | |
| G200_RS0101695 | 2.56366058 | 1.13E-09 | Major myo-inositol transporter IolT |
| G200_RS0103410 | 2.81622077 | 3.38E-45 | Inosose dehydratase IolE |

| | | | |
|---|---|---|---|
| G200_RS0103415 | 3.051765216 | 2.74E-47 | Glyceraldehyde-3-phosphate ketol-isomerase IolH |
| G200_RS0103420 | 3.612129551 | 3.41E-57 | Myo-inositol 2-dehydrogenase 1 IolG |
| G200_RS0103425 | 3.034782963 | 1.24E-11 | Epi-inositol hydrolase IolD |
| G200_RS0103430 | 2.455264684 | 4.22E-08 | 5-keto-2-deoxygluconokinase IolC |
| G200_RS0103435 | 1.82595615 | 7.10E-18 | Transcriptional regulator of the myo-inositol catabolic operon IolR |
| G200_RS0103440 | 2.322930823 | 6.16E-29 | 5-deoxy-glucuronate isomerase IolB |
| G200_RS0103445 | 2.343048715 | 1.92E-08 | Methylmalonate-semialdehyde dehydrogenase IolA |
| G200_RS0103450 | 2.393433177 | 3.58E-08 | Inosose isomerase IolI |
| G200_RS0103485 | 2.265947451 | 7.57E-22 | Inosose dehydratase |
| G200_RS0103490 | 1.606575527 | 5.42E-13 | Myo-inositol 2-dehydrogenase |
| G200_RS0109945 | 2.054104613 | 1.56E-06 | Myo-inositol 2-dehydrogenase |
| G200_RS0111735 | 2.826752946 | 1.30E-21 | Major myo-inositol transporter IolT |
| G200_RS0119935 | 2.36064358 | 6.17E-31 | Inositol transport system permease protein |
| G200_RS0119940 | 2.922693363 | 5.94E-43 | Inositol transport system ATP-binding protein |
| G200_RS0119945 | 2.723773939 | 6.09E-34 | Inositol transport system sugar-binding protein |
| G200_RS0120045 | 2.507147476 | 1.44E-09 | Myo-inositol 2-dehydrogenase 2 |
| D-galactarate, D-glucarate and D-glycerate catabolism | | | |
| G200_RS0114355 | -1.471923639 | 1.25E-06 | MFS transporter |
| G200_RS0124280 | -2.146858379 | 7.57E-39 | D-galactarate dehydratase GarD |
| G200_RS0124290 | -2.155286292 | 3.22E-65 | D-glucarate permease |
| G200_RS0124295 | -1.762097381 | 2.90E-22 | Glucarate dehydratase GudD |
| G200_RS0124300 | -1.801096855 | 3.95E-16 | Glucarate dehydratase GudD |
| G200_RS0124305 | -1.841655614 | 7.57E-39 | 2-dehydro-3-deoxyglucarate aldolase GarL |
| G200_RS0124320 | -1.921850417 | 2.06E-49 | Glycerate kinase |
| G200_RS25820 | -2.073060541 | 9.97E-53 | 3-hydroxyisobutyrate dehydrogenase GarR |
| Maltose and Maltodextrin catabolism | | | |
| G200_RS0105520 | -1.474187006 | 1.51E-22 | PTS system, maltose and glucose-specific IIABC component |
| G200_RS0114455 | -2.146215061 | 6.10E-08 | Maltose/maltodextrin high-affinity receptor LamB |
| G200_RS0114460 | -3.460976388 | 1.17E-46 | Maltose/maltodextrin transport ATP-binding protein MalK |
| G200_RS0114465 | -3.432632153 | 3.66E-74 | Maltose/maltodextrin ABC transporter, substrate binding periplasmic protein MalE |
| G200_RS0114470 | -1.356395147 | 1.92E-06 | Maltose ABC transporter permease MalF |

| | | | |
|---|---|---|---|
| Other carbohydrates metabolism | | | |
| G200_RS0102345 | -1.326068817 | 1.39E-19 | 6-phospho-beta-glucosidase |
| G200_RS0120860 | -1.385897754 | 2.78E-07 | PTS beta-glucoside transporter subunit EIIBCA |
| G200_RS0109880 | 1.195365256 | 3.02E-14 | Beta-glucuronidase |
| G200_RS0108005 | 1.553737025 | 2.47E-29 | Alcohol dehydrogenase |
| G200_RS0118365 | 1.430810069 | 6.79E-14 | Pyruvate formate-lyase |
| G200_RS0108900 | 1.148093171 | 1.24E-10 | Deoxyribose-phosphate aldolase |
| G200_RS0116155 | 1.055489576 | 4.73E-12 | Ribokinase |
| G200_RS0109855 | 1.1278524 | 1.96E-13 | Mannonate dehydratase |
| G200_RS0102390 | 2.327906926 | 3.00E-11 | Gluconate 2-dehydrogenase, membrane-bound, flavoprotein |
| G200_RS0102395 | 2.004607764 | 1.22E-17 | Gluconate 2-dehydrogenase, membrane-bound, gamma subunit |
| G200_RS0119505 | 1.507781586 | 2.74E-15 | Ribose ABC transport system, periplasmic ribose-binding protein RbsB |
| G200_RS0118360 | 1.344548034 | 3.43E-28 | Pyruvate formate lyase 1-activating protein PflA |
| G200_RS0121040 | 1.68097694 | 2.43E-04 | Aerobic glycerol-3-phosphate dehydrogenase GlpD |
| G200_RS0121025 | -1.369452767 | 7.02E-22 | Glucose-1-phosphate adenylyltransferase GlgC |
| G200_RS0121030 | -1.413808857 | 4.42E-26 | Glycogen synthase GlgA |
| G200_RS0108965 | 1.651181716 | 2.59E-16 | 6-phosphofructokinase |
| G200_RS0105430 | -1.010271981 | 3.98E-16 | Aconitate hydratase AcnA |
| G200_RS0114595 | -1.302381077 | 1.85E-17 | Malate synthase |
| G200_RS0101545 | -2.502124169 | 2.13E-42 | L-lactate dehydrogenase |
| G200_RS0109845 | 1.012221802 | 6.78E-09 | MFS transporter LacY |
| G200_RS0118000 | 1.499549769 | 9.33E-05 | 6-phosphogluconolactonase |
| G200_RS0100900 | -1.050323621 | 2.49E-14 | DUF485 domain-containing protein |
| G200_RS0100905 | -1.143638292 | 2.68E-11 | Cation/acetate symporter ActP |
| G200_RS0121020 | -1.529478972 | 2.20E-39 | Glycogen debranching enzyme |
| G200_RS0113990 | 1.292475653 | 5.30E-11 | PTS sugar transporter subunit IIB |
| G200_RS0113995 | 1.209666009 | 1.43E-15 | Putative carbohydrate PTS system, IIA component |
| G200_RS0114000 | 1.458640254 | 1.69E-13 | Putative transcriptional regulator of unknown carbohydrate utilization cluster, GntR family |
| G200_RS0104280 | -1.044495518 | 3.39E-06 | Alpha/beta hydrolase |
| **Gene ID** | **$log_2$(ETEOI/ET)** | **FDR** | **Gene product** |

| | | | |
|---|---|---|---|
| Inositol catabolism | | | |
| G200_RS010169 5 | 2.56366058 | 1.13E-09 | Major myo-inositol transporter IolT |
| G200_RS010341 0 | 2.81622077 | 3.38E-45 | Inosose dehydratase IolE |
| G200_RS010341 5 | 3.051765216 | 2.74E-47 | Glyceraldehyde-3-phosphate ketol-isomerase IolH |
| G200_RS010342 0 | 3.612129551 | 3.41E-57 | Myo-inositol 2-dehydrogenase 1 IolG |
| G200_RS010342 5 | 3.034782963 | 1.24E-11 | Epi-inositol hydrolase IolD |
| G200_RS010343 0 | 2.455264684 | 4.22E-08 | 5-keto-2-deoxygluconokinase IolC |
| G200_RS010343 5 | 1.82595615 | 7.10E-18 | Transcriptional regulator of the myo-inositol catabolic operon IolR |
| G200_RS010344 0 | 2.322930823 | 6.16E-29 | 5-deoxy-glucuronate isomerase IolB |
| G200_RS010344 5 | 2.343048715 | 1.92E-08 | Methylmalonate-semialdehyde dehydrogenase IolA |
| G200_RS010345 0 | 2.393433177 | 3.58E-08 | Inosose isomerase IolI |
| G200_RS010348 5 | 2.265947451 | 7.57E-22 | Inosose dehydratase |
| G200_RS010349 0 | 1.606575527 | 5.42E-13 | Myo-inositol 2-dehydrogenase |
| G200_RS010994 5 | 2.054104613 | 1.56E-06 | Myo-inositol 2-dehydrogenase |
| G200_RS011173 5 | 2.826752946 | 1.30E-21 | Major myo-inositol transporter IolT |
| G200_RS011993 5 | 2.36064358 | 6.17E-31 | Inositol transport system permease protein |
| G200_RS011994 0 | 2.922693363 | 5.94E-43 | Inositol transport system ATP-binding protein |
| G200_RS011994 5 | 2.723773939 | 6.09E-34 | Inositol transport system sugar-binding protein |
| G200_RS012004 5 | 2.507147476 | 1.44E-09 | Myo-inositol 2-dehydrogenase 2 |
| D-galactarate, D-glucarate and D-glycerate catabolism | | | |
| G200_RS011435 5 | -1.471923639 | 1.25E-06 | MFS transporter |
| G200_RS012428 0 | -2.146858379 | 7.57E-39 | D-galactarate dehydratase GarD |
| G200_RS012429 0 | -2.155286292 | 3.22E-65 | D-glucarate permease |
| G200_RS012429 5 | -1.762097381 | 2.90E-22 | Glucarate dehydratase GudD |
| G200_RS012430 0 | -1.801096855 | 3.95E-16 | Glucarate dehydratase GudD |
| G200_RS012430 5 | -1.841655614 | 7.57E-39 | 2-dehydro-3-deoxyglucarate aldolase GarL |
| G200_RS012432 0 | -1.921850417 | 2.06E-49 | Glycerate kinase |
| G200_RS25820 | -2.073060541 | 9.97E-53 | 3-hydroxyisobutyrate dehydrogenase GarR |
| Maltose and Maltodextrin catabolism | | | |
| G200_RS010552 0 | -1.474187006 | 1.51E-22 | PTS system, maltose and glucose-specific IIABC component |
| G200_RS011445 5 | -2.146215061 | 6.10E-08 | Maltose/maltodextrin high-affinity receptor LamB |

| | | | |
|---|---|---|---|
| G200_RS011446 0 | -3.460976388 | 1.17E-46 | Maltose/maltodextrin transport ATP-binding protein MalK |
| G200_RS011446 5 | -3.432632153 | 3.66E-74 | Maltose/maltodextrin ABC transporter, substrate binding periplasmic protein MalE |
| G200_RS011447 0 | -1.356395147 | 1.92E-06 | Maltose ABC transporter permease MalF |
| Other carbohydrates metabolism | | | |
| G200_RS010234 5 | -1.326068817 | 1.39E-19 | 6-phospho-beta-glucosidase |
| G200_RS012086 0 | -1.385897754 | 2.78E-07 | PTS beta-glucoside transporter subunit EIIBCA |
| G200_RS010988 0 | 1.195365256 | 3.02E-14 | Beta-glucuronidase |
| G200_RS010800 5 | 1.553737025 | 2.47E-29 | Alcohol dehydrogenase |
| G200_RS011836 5 | 1.430810069 | 6.79E-14 | Pyruvate formate-lyase |
| G200_RS010890 0 | 1.148093171 | 1.24E-10 | Deoxyribose-phosphate aldolase |
| G200_RS011615 5 | 1.055489576 | 4.73E-12 | Ribokinase |
| G200_RS010985 5 | 1.1278524 | 1.96E-13 | Mannonate dehydratase |
| G200_RS010239 0 | 2.327906926 | 3.00E-11 | Gluconate 2-dehydrogenase, membrane-bound, flavoprotein |
| G200_RS010239 5 | 2.004607764 | 1.22E-17 | Gluconate 2-dehydrogenase, membrane-bound, gamma subunit |
| G200_RS011950 5 | 1.507781586 | 2.74E-15 | Ribose ABC transport system, periplasmic ribose-binding protein RbsB |
| G200_RS011836 0 | 1.344548034 | 3.43E-28 | Pyruvate formate lyase 1-activating protein PflA |
| G200_RS012104 0 | 1.68097694 | 2.43E-04 | Aerobic glycerol-3-phosphate dehydrogenase GlpD |
| G200_RS012102 5 | -1.369452767 | 7.02E-22 | Glucose-1-phosphate adenylyltransferase GlgC |
| G200_RS012103 0 | -1.413808857 | 4.42E-26 | Glycogen synthase GlgA |
| G200_RS010896 5 | 1.651181716 | 2.59E-16 | 6-phosphofructokinase |
| G200_RS010543 0 | -1.010271981 | 3.98E-16 | Aconitate hydratase AcnA |
| G200_RS011459 5 | -1.302381077 | 1.85E-17 | Malate synthase |
| G200_RS010154 5 | -2.502124169 | 2.13E-42 | L-lactate dehydrogenase |
| G200_RS010984 5 | 1.012221802 | 6.78E-09 | MFS transporter LacY |
| G200_RS011800 0 | 1.499549769 | 9.33E-05 | 6-phosphogluconolactonase |
| G200_RS010090 0 | -1.050323621 | 2.49E-14 | DUF485 domain-containing protein |
| G200_RS010090 5 | -1.143638292 | 2.68E-11 | Cation/acetate symporter ActP |
| G200_RS012102 0 | -1.529478972 | 2.20E-39 | Glycogen debranching enzyme |
| G200_RS011399 0 | 1.292475653 | 5.30E-11 | PTS sugar transporter subunit IIB |
| G200_RS011399 5 | 1.209666009 | 1.43E-15 | Putative carbohydrate PTS system, IIA component |

| | | | |
|---|---|---|---|
| G200_RS0114000 | 1.458640254 | 1.69E-13 | Putative transcriptional regulator of unknown carbohydrate utilization cluster, GntR family |
| G200_RS0104280 | -1.044495518 | 3.39E-06 | Alpha/beta hydrolase |

## References

1. Bulgarelli D, Schlaeppi K, Spaepen S, Ver Loren van Themaat E, Schulze-Lefert P. 2013. Structure and functions of the bacterial microbiota of plants. Annu Rev Plant Biol 64:807-38.
2. Schlaeppi K, Bulgarelli D. 2015. The plant microbiome at work. Mol Plant Microbe Interact 28:212-7.
3. Fuqua WC, Winans SC, Greenberg EP. 1994. Quorum sensing in bacteria: the LuxR-LuxI family of cell density-responsive transcriptional regulators. J Bacteriol 176:269-75.
4. Miller MB, Bassler BL. 2001. Quorum sensing in bacteria. Annu Rev Microbiol 55:165-99.
5. Cha C, Gao P, Chen YC, Shaw PD, Farrand SK. 1998. Production of acyl-homoserine lactone quorum-sensing signals by gram-negative plant-associated bacteria. Mol Plant Microbe Interact 11:1119-29.
6. Danhorn T, Fuqua C. 2007. Biofilm formation by plant-associated bacteria. Annu Rev Microbiol 61:401-22.
7. Gonzalez JE, Marketon MM. 2003. Quorum sensing in nitrogen-fixing rhizobia. Microbiol Mol Biol Rev 67:574-92.
8. Newton JA, Fray RG. 2004. Integration of environmental and host-derived signals with quorum sensing during plant-microbe interactions. Cell Microbiol 6:213-24.
9. Von Bodman SB, Bauer WD, Coplin DL. 2003. Quorum sensing in plant-pathogenic bacteria. Annu Rev Phytopathol 41:455-82.
10. Fuqua C, Parsek MR, Greenberg EP. 2001. Regulation of gene expression by cell-to-cell communication: acyl-homoserine lactone quorum sensing. Annu Rev Genet 35:439-68.
11. Lamichhane JR, Venturi V. 2015. Synergisms between microbial pathogens in plant disease complexes: a growing trend. Front Plant Sci 6:385.
12. Vayssier-Taussat M, Albina E, Citti C, Cosson JF, Jacques MA, Lebrun MH, Le Loir Y, Ogliastro M, Petit MA, Roumagnac P, Candresse T. 2014. Shifting the paradigm from pathogens to pathobiome: new concepts in the light of meta-omics. Front Cell Infect Microbiol 4:29.
13. Venturi V, da Silva DP. 2012. Incoming pathogens team up with harmless 'resident' bacteria. Trends Microbiol 20:160-4.
14. Buonaurio R, Moretti C, da Silva DP, Cortese C, Ramos C, Venturi V. 2015. The olive knot disease as a model to study the role of interspecies bacterial communities in plant disease. Front Plant Sci 6:434.
15. Hosni T, Moretti C, Devescovi G, Suarez-Moreno ZR, Fatmi MB, Guarnaccia C, Pongor S, Onofri A, Buonaurio R, Venturi V. 2011. Sharing of quorum-sensing signals and role of interspecies communities in a bacterial plant disease. ISME J 5:1857-70.
16. Passos da Silva D, Castaneda-Ojeda MP, Moretti C, Buonaurio R, Ramos C, Venturi V. 2014. Bacterial multispecies studies and microbiome analysis of a plant disease. Microbiology 160:556-66.

17. Perez-Martinez I, Rodriguez-Moreno L, Matas IM, Ramos C. 2007. Strain selection and improvement of gene transfer for genetic manipulation of *Pseudomonas savastanoi* isolated from olive knots. Res Microbiol 158:60-9.
18. Perez-Martinez I, Rodriguez-Moreno L, Lambertsen L, Matas IM, Murillo J, Tegli S, Jimenez AJ, Ramos C. 2010. Fate of a *Pseudomonas savastanoi* pv. *savastanoi* type III secretion system mutant in olive plants (Olea europaea L.). Appl Environ Microbiol.
19. Rodriguez-Palenzuela P, Matas IM, Murillo J, Lopez-Solanilla E, Bardaji L, Perez-Martinez I, Rodriguez-Moskera ME, Penyalver R, Lopez MM, Quesada JM, Biehl BS, Perna NT, Glasner JD, Cabot EL, Neeno-Eckwall E, Ramos C. 2010. Annotation and overview of the *Pseudomonas savastanoi* pv. *savastanoi* NCPPB 3335 draft genome reveals the virulence gene complement of a tumour-inducing pathogen of woody hosts. Environ Microbiol 12:1604-1620.
20. Subramoni S, Florez Salcedo DV, Suarez-Moreno ZR. 2015. A bioinformatic survey of distribution, conservation, and probable functions of LuxR solo regulators in bacteria. Front Cell Infect Microbiol 5:16.
21. Subramoni S, Venturi V. 2009. LuxR-family 'solos': bachelor sensors/regulators of signalling molecules. Microbiology 155:1377-85.
22. Moretti C, Cortese C, Passos da Silva D, Venturi V, Ramos C, Firrao G, Buonaurio R. 2014. Draft Genome Sequence of Pseudomonas savastanoi pv. savastanoi Strain DAPP-PG 722, Isolated in Italy from an Olive Plant Affected by Knot Disease. Genome Announc 2.
23. Moretti C, Cortese C, Passos da Silva D, Venturi V, Torelli E, Firrao G, Buonaurio R. 2014. Draft Genome Sequence of a Hypersensitive Reaction-Inducing Pantoea agglomerans Strain Isolated from Olive Knots Caused by *Pseudomonas savastanoi* pv. *savastanoi*. Genome Announc 2.
24. Bartoli C, Carrere S, Lamichhane JR, Varvaro L, Morris CE. 2015. Whole-Genome Sequencing of 10 Pseudomonas syringae Strains Representing Different Host Range Spectra. Genome Announc 3.
25. Thakur S, Weir BS, Guttman DS. 2016. Phytopathogen Genome Announcement: Draft Genome Sequences of 62 Pseudomonas syringae Type and Pathotype Strains. Mol Plant Microbe Interact 29:243-6.
26. Passos da Silva D, Devescovi G, Paszkiewicz K, Moretti C, Buonaurio R, Studholme DJ, Venturi V. 2013. Draft Genome Sequence of Erwinia toletana, a Bacterium Associated with Olive Knots Caused by Pseudomonas savastanoi pv. Savastanoi. Genome Announc 1:e00205-13.
27. Huynh TV, Dahlbeck D, Staskawicz BJ. 1989. Bacterial blight of soybean: regulation of a pathogen gene determining host cultivar specificity. Science 245:1374-7.
28. Yu X, Lund SP, Greenwald JW, Records AH, Scott RA, Nettleton D, Lindow SE, Gross DC, Beattie GA. 2014. Transcriptional analysis of the global regulatory networks active in *Pseudomonas syringae* during leaf colonization. MBio 5:e01683-14.
29. Venturi V, Passos da Silva D. 2012. Incoming pathogens team up with harmless 'resident' bacteria. Trends Microbiol 20:160-164.

30. Deng X, Xiao Y, Lan L, Zhou JM, Tang X. 2009. *Pseudomonas syringae* pv. *phaseolicola* mutants compromised for type III secretion system gene induction. Mol Plant Microbe Interact 22:964-76.

31. Quinones B, Pujol CJ, Lindow SE. 2004. Regulation of AHL production and its contribution to epiphytic fitness in *Pseudomonas syringae*. Mol Plant Microbe Interact 17:521-31.

32. Chalupowicz L, Barash I, Panijel M, Sessa G, Manulis-Sasson S. 2009. Regulatory interactions between quorum-sensing, auxin, cytokinin, and the Hrp regulon in relation to gall formation and epiphytic fitness of *Pantoea agglomerans* pv. *gypsophilae*. Mol Plant Microbe Interact 22:849-56.

33. Dulla G, Lindow SE. 2008. Quorum size of *Pseudomonas syringae* is small and dictated by water availability on the leaf surface. Proc Natl Acad Sci U S A 105:3082-7.

34. Whitehead NA, Barnard AM, Slater H, Simpson NJ, Salmond GP. 2001. Quorum-sensing in Gram-negative bacteria. FEMS Microbiol Rev 25:365-404.

35. Cheng F, Ma A, Luo J, Zhuang X, Zhuang G. 2017. N-acylhomoserine lactone-regulation of genes mediating motility and pathogenicity in *Pseudomonas syringae* pathovar *tabaci* 11528. Microbiologyopen 6.

36. Scott RA, Lindow SE. 2016. Transcriptional control of quorum sensing and associated metabolic interactions in *Pseudomonas syringae* strain B728a. Mol Microbiol 99:1080-98.

37. Barnard AM, Salmond GP. 2007. Quorum sensing in *Erwinia* species. Anal Bioanal Chem 387:415-23.

38. Sibanda S, Theron J, Shyntum DY, Moleleki LN, Coutinho TA. 2016. Characterization of two LuxI/R homologs in *Pantoea ananatis* LMG 2665T. Can J Microbiol 62:893-903.

39. Zheng H, Mao Y, Zhu Q, Ling J, Zhang N, Naseer N, Zhong Z, Zhu J. 2015. The quorum sensing regulator CinR hierarchically regulates two other quorum sensing pathways in ligand-dependent and -independent fashions in *Rhizobium etli*. J Bacteriol 197:1573-81.

40. Mattiuzzo M, Bertani I, Ferluga S, Cabrio L, Bigirimana J, Guarnaccia C, Pongor S, Maraite H, Venturi V. 2011. The plant pathogen *Pseudomonas fuscovaginae* contains two conserved quorum sensing systems involved in virulence and negatively regulated by RsaL and the novel regulator RsaM. Environ Microbiol 13:145-62.

41. Liu X, Jia J, Popat R, Ortori CA, Li J, Diggle SP, Gao K, Camara M. 2011. Characterisation of two quorum sensing systems in the endophytic *Serratia plymuthica* strain G3: differential control of motility and biofilm formation according to life-style. BMC Microbiol 11:26.

42. Venturi V. 2006. Regulation of quorum sensing in *Pseudomonas*. FEMS Microbiol Rev 30:274-91.

43. Barka EA, Belarbi A, Hachet C, Nowak J, Audran JC. 2000. Enhancement of in vitro growth and resistance to gray mould of *Vitis vinifera* co-cultured with plant growth-promoting rhizobacteria. FEMS Microbiol Lett 186:91-5.

44. Hubbard BK, Koch M, Palmer DR, Babbitt PC, Gerlt JA. 1998. Evolution of enzymatic activities in the enolase superfamily: characterization of the (D)-

glucarate/galactarate catabolic pathway in *Escherichia coli*. Biochemistry 37:14369-75.

45. Miller JH. 1972. Experiments in molecular genetics, Cold Spring Harbor, N.Y.
46. Hanahan D. 1983. Studies on transformation of *Escherichia coli* with plasmids. J Mol Biol 166:557-80.
47. Sambrook J, Fritsch EF, Maniatis T. 1989. Molecular cloning: a laboratory manual, 2nd ed., Cold Spring Harbor, N.Y.
48. Matas IM, Castaneda-Ojeda MP, Aragon IM, Antunez-Lamas M, Murillo J, Rodriguez-Palenzuela P, Lopez-Solanilla E, Ramos C. 2014. Translocation and functional analysis of *Pseudomonas savastanoi* pv. *savastanoi* NCPPB 3335 type III secretion system effectors reveals two novel effector families of the *Pseudomonas syringae* complex. Mol Plant Microbe Interact 27:424-36.
49. Aragon IM, Perez-Martinez I, Moreno-Perez A, Cerezo M, Ramos C. 2014. New insights into the role of indole-3-acetic acid in the virulence of *Pseudomonas savastanoi* pv. *savastanoi*. FEMS Microbiol Lett 356:184-92.
50. Alexeyev MF. 1999. The pKNOCK series of broad-host-range mobilizable suicide vectors for gene knockout and targeted DNA insertion into the chromosome of gram-negative bacteria. Biotechniques 26:824-6, 828.
51. Coutinho BG, Mitter B, Talbi C, Sessitsch A, Bedmar EJ, Halliday N, James EK, Camara M, Venturi V. 2013. Regulon studies and in planta role of the BraI/R quorum sensing system in the plant beneficial Burkholderia cluster. Appl Environ Microbiol 79:4421-4432.
52. Spaink HP, Okker RJH, Wijffelmann CA, Pees E, Lugtemberg BJJ. 1987. Promoter in the nodulation region of the *Rhizobium leguminosarum* Sym plasmid pRL1JI. Plant Mol Biol 9:27-39.
53. Uzelac G, Patel HK, Devescovi G, Licastro D, Venturi V. 2017. Quorum sensing and RsaM regulons of the rice pathogen *Pseudomonas fuscovaginae*. Microbiology in press.
54. Choi SK, Matsuda S, Hoshino T, Peng X, Misawa N. 2006. Characterization of bacterial beta-carotene 3,3'-hydroxylases, CrtZ, and P450 in astaxanthin biosynthetic pathway and adonirubin production by gene combination in *Escherichia coli*. Appl Microbiol Biotechnol 72:1238-46.
55. Vezzi F, Del Fabbro C, Tomescu AI, Policriti A. 2012. rNA: a fast and accurate short reads numerical aligner. Bioinformatics 28:123-4.
56. Altschul SF, Gish W, Miller W, Myers EW, Lipman DJ. 1990. Basic local alignment search tool. J Mol Biol 215:403-10.
57. Trapnell C, Hendrickson DG, Sauvageau M, Goff L, Rinn JL, Pachter L. 2013. Differential analysis of gene regulation at transcript resolution with RNA-seq. Nat Biotechnol 31:46-53.
58. Trapnell C, Roberts A, Goff L, Pertea G, Kim D, Kelley DR, Pimentel H, Salzberg SL, Rinn JL, Pachter L. 2012. Differential gene and transcript expression analysis of RNA-seq experiments with TopHat and Cufflinks. Nat Protoc 7:562-78.
59. Benjamini Y, Hochberg Y. 1995. Controlling the false discovery rate: a practical and powerful approach to multiple testing J Royal Stat Soc 57:289-300.

60. Thornton B, Basu C. 2011. Real-time PCR (qPCR) primer design using free online software. Biochem Mol Biol Educ 39:145-54.

61. Livak KJ, Schmittgen TD. 2001. Analysis of relative gene expression data using real-time quantitative PCR and the 2(-Delta Delta C(T)) Method. Methods 25:402-8.

62. Rodriguez-Moreno L, Barcelo-Munoz A, Ramos C. 2008. In vitro analysis of the interaction of *Pseudomonas savastanoi* pvs. *savastanoi* and *nerii* with micropropagated olive plants. Phytopathology 98:815-22.

63. Matas IM, Lambertsen L, Rodriguez-Moreno L, Ramos C. 2012. Identification of novel virulence genes and metabolic pathways required for full fitness of *Pseudomonas savastanoi* pv. *savastanoi* in olive (*Olea europaea*) knots. New Phytol 196:1182-96.

64. Penyalver R, Garcia A, Ferrer A, Bertolini E, Quesada JM, Salcedo CI, Piquer J, Perez-Panades J, Carbonell EA, Del Rio C, Caballero JM, Lopez MM. 2006. Factors affecting *Pseudomonas savastanoi* pv. *savastanoi* plant Inoculations and their use for evaluation of olive cultivar susceptibility. Phytopathology 96:313-9.

65. Moretti C, Ferrante P, Hosni T, Valentini F, D'Onghia A, Fatmi M, Buonaurio R. 2008. Characterization of *Pseudomonas savastanoi* pv. *savastanoi* strains collected from olive trees from different countries. *In* M'Barek Fatmi AC, Nicola Sante Iacobellis, John W. Mansfield, Jesus Murillo, Norman W. Schaad and Matthias Ullrich (ed), *Pseudomonas syringae* Pathovars and Related Pathogens - Identification, Epidemiology and Genomics. Springer Netherlands.

66. Simon R, Priefer U, Puhler A. 1983. A broad host range mobilization system for *in vivo* genetic engineering: transposon mutagenesis in Gram negative bacteria. Nat Biotech 1:784-791.

67. Rodriguez-Moreno L, Jimenez AJ, Ramos C. 2009. Endopathogenic lifestyle of *Pseudomonas savastanoi* pv. *savastanoi* in olive knots. Microb Biotechnol 2:476-488.

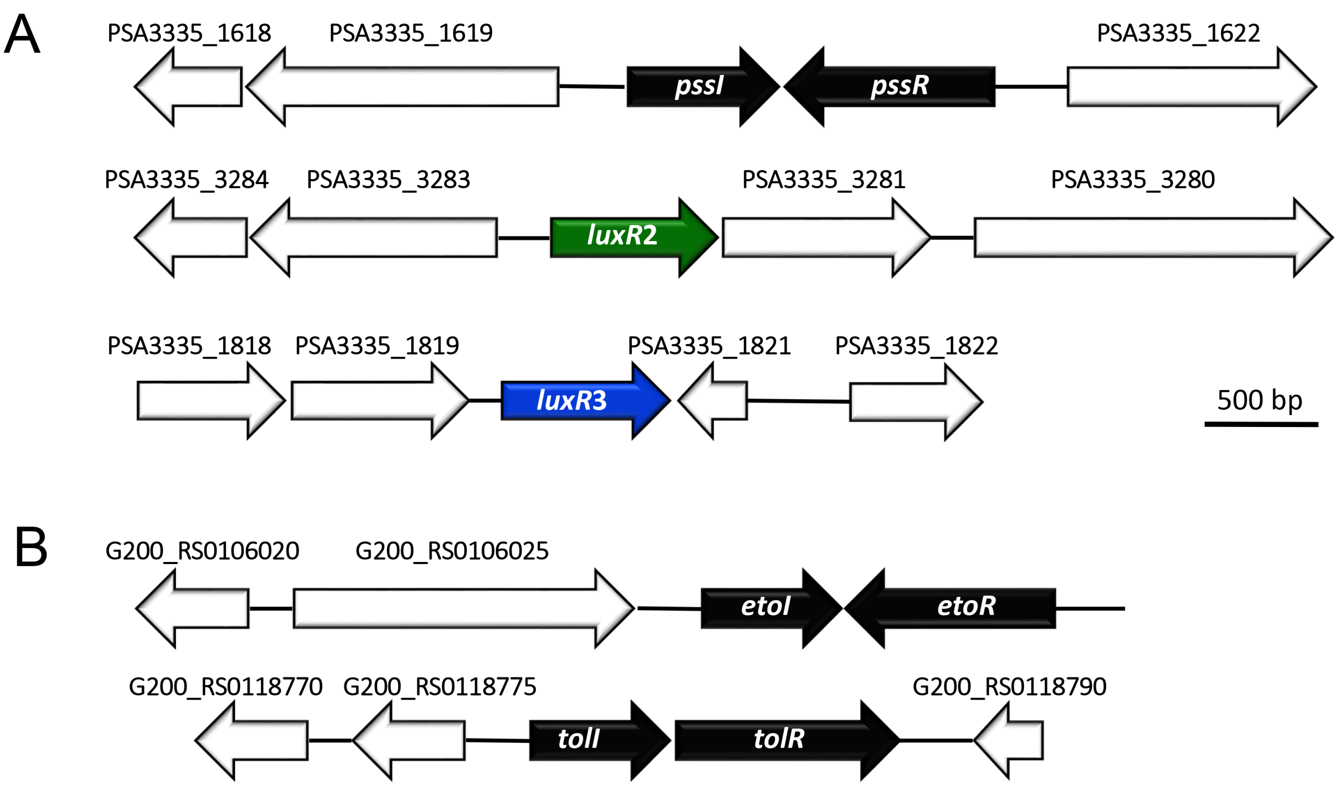
A
PSA3335_1618
PSA3335_1619
pssI
pssR
PSA3335_1622
PSA3335_3284
PSA3335_3283
luxR2
PSA3335_3281
PSA3335_3280
PSA3335_1818
PSA3335_1819
luxR3
PSA3335_1821
PSA3335_1822
500 bp
B
G200_RS0106020
G200_RS0106025
etoI
etoR
G200_RS0118770
G200_RS0118775
tolI
tolR
G200_RS0118790

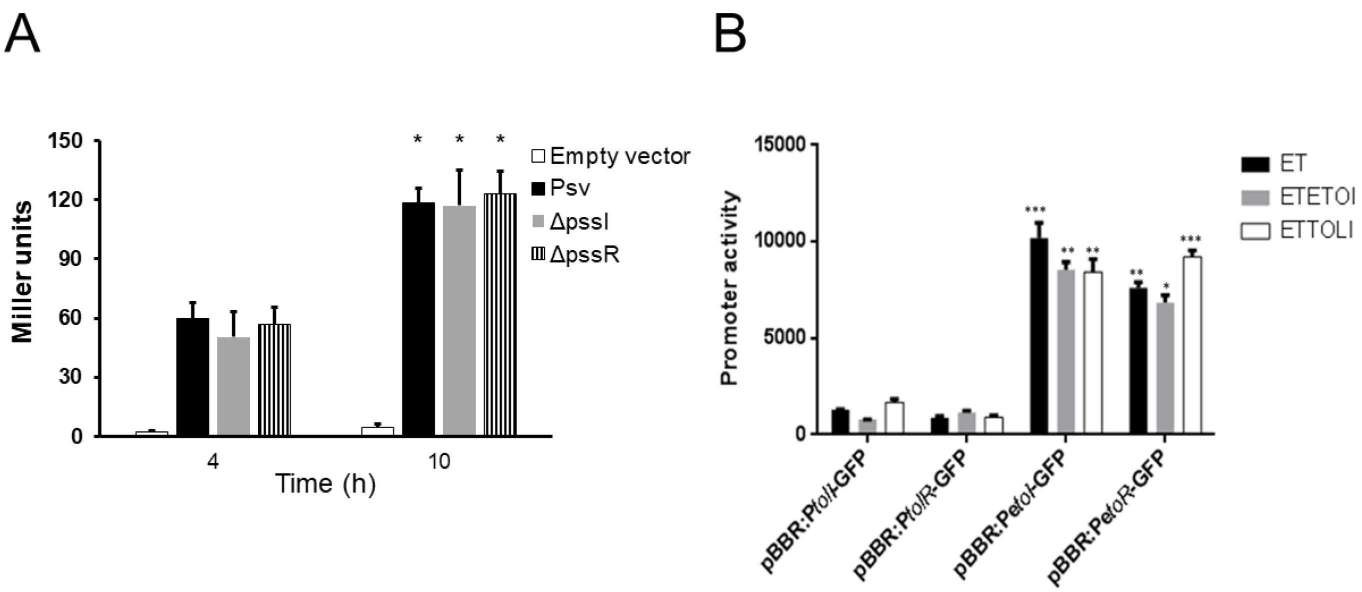
A
150
120
90
60
30
0
Miller units
*
*
*
Empty vector
Psv
ΔpssI
ΔpssR
4
10
Time (h)
B
15000
10000
5000
0
Promoter activity
ET
ETETOI
ETTOLI
***
**
**
**
*
***
pBBR:PtolI-GFP
pBBR:PtolR-GFP
pBBR:PetoI-GFP
pBBR:PetoR-GFP

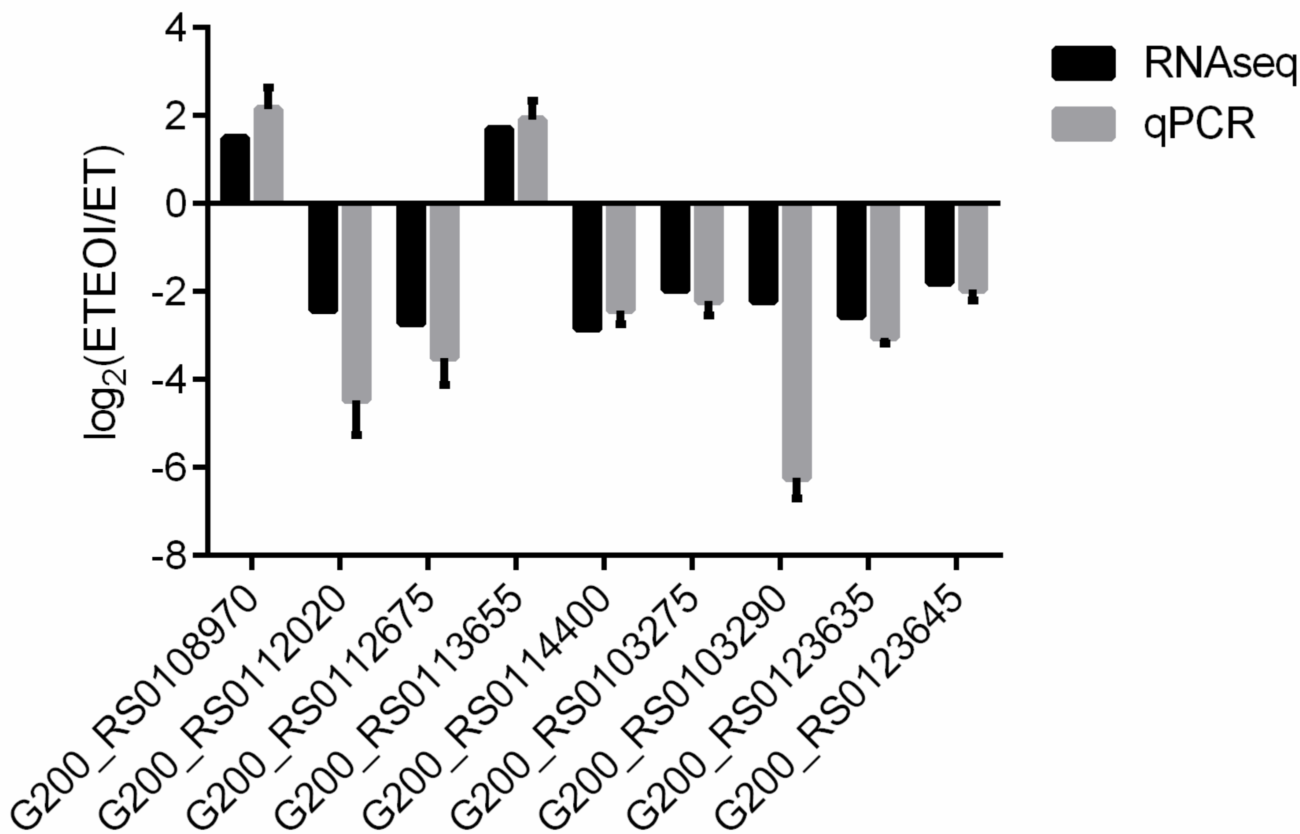
RNAseq
qPCR
log2(ETEOI/ET)
4
2
0
-2
-4
-6
-8
G200_RS0108970
G200_RS0112020
G200_RS0112675
G200_RS0113655
G200_RS0114400
G200_RS0103275
G200_RS0103290
G200_RS0123635
G200_RS0123645

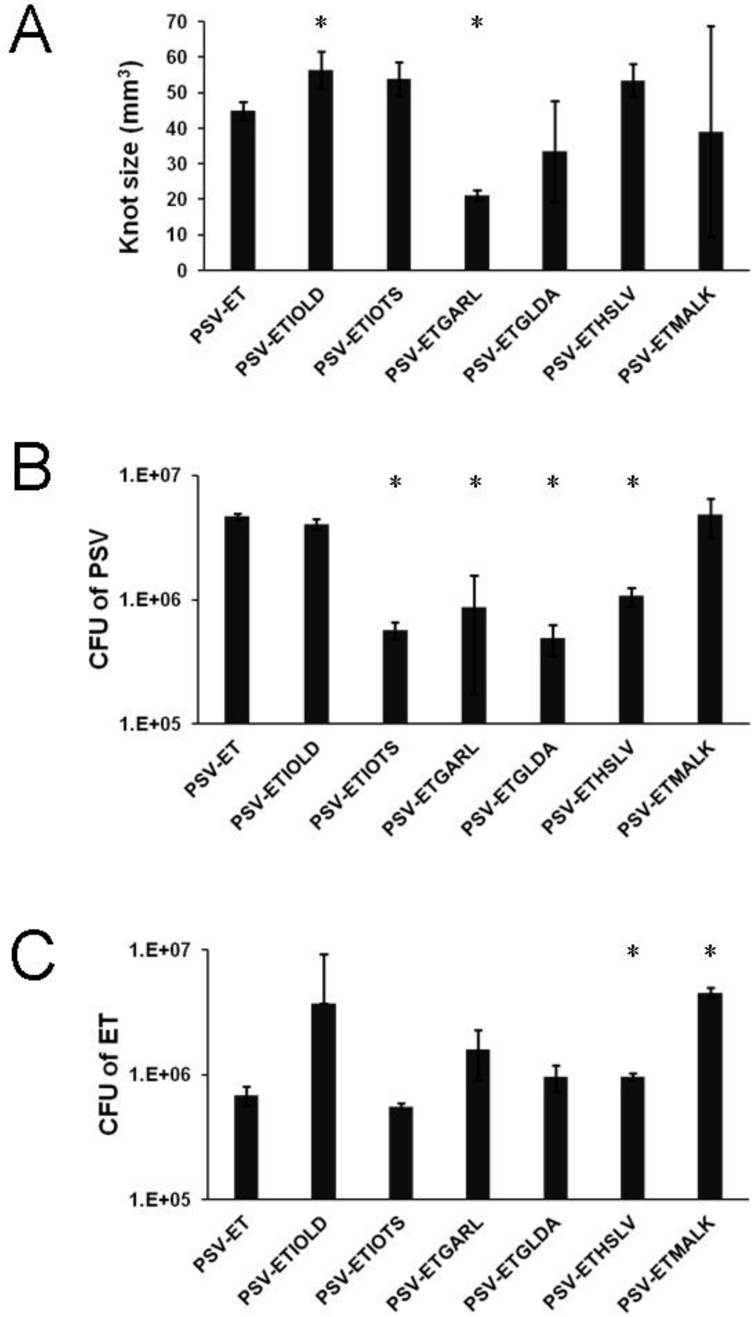
A
Knot size (mm3)
0
10
20
30
40
50
60
70
*
*
PSV-ET
PSV-ETIOLD
PSV-ETIOTS
PSV-ETGARL
PSV-ETGLDA
PSV-ETHSLV
PSV-ETMALK
B
CFU of PSV
1.E+05
1.E+06
1.E+07
*
*
*
*
PSV-ET
PSV-ETIOLD
PSV-ETIOTS
PSV-ETGARL
PSV-ETGLDA
PSV-ETHSLV
PSV-ETMALK
C
CFU of ET
1.E+05
1.E+06
1.E+07
*
*
PSV-ET
PSV-ETIOLD
PSV-ETIOTS
PSV-ETGARL
PSV-ETGLDA
PSV-ETHSLV
PSV-ETMALK

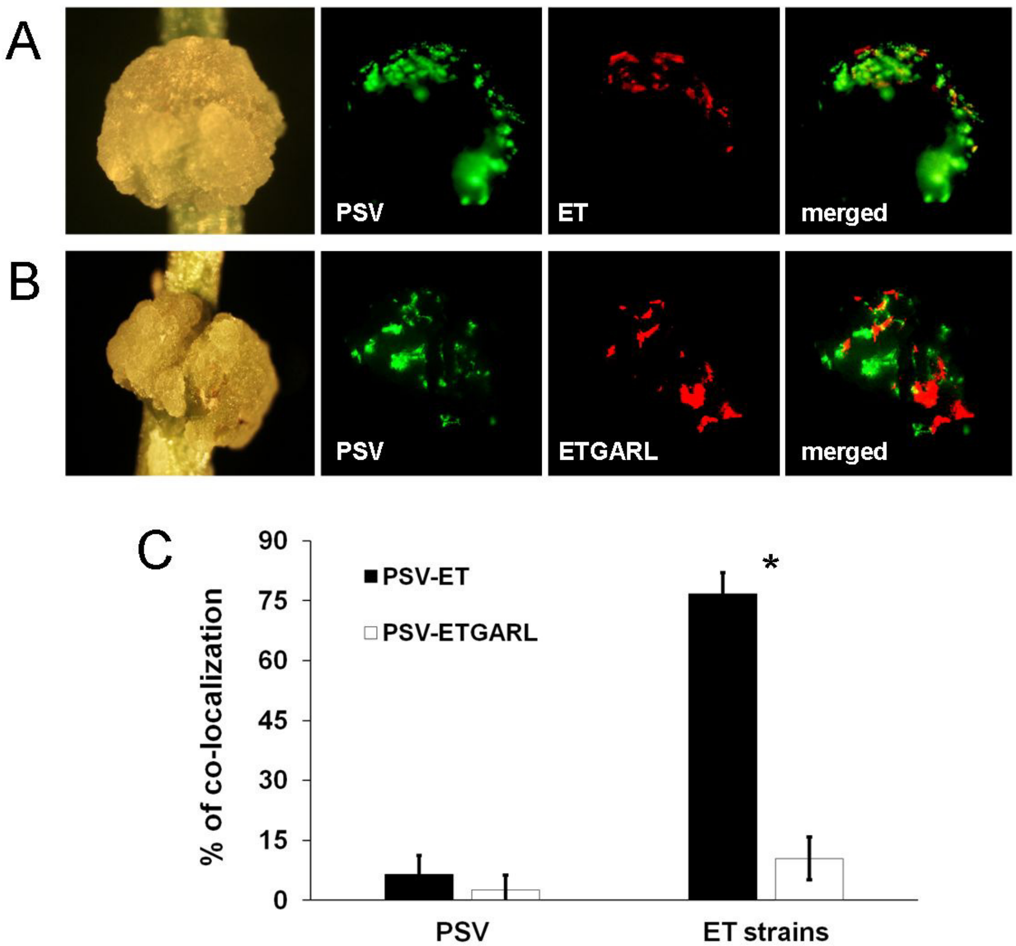
A
PSV
ET
merged
B
PSV
ETGARL
merged
C
90
75
60
45
30
15
0
% of co-localization
PSV-ET
PSV-ETGARL
*
PSV
ET strains